# UNIVERSIDAD DE INVESTIGACIÓN DE TECNOLOGÍA EXPERIMENTAL YACHAY

**Escuela de Ciencias Físicas y Nanotecnología**

# TÍTULO: EMBEDDED CERIA NANOPARTICLES IN BIOPOLYMER ELECRTOSPUN FIBERS FOR BIOMEDICAL APPLICATIONS

Trabajo de integración curricular presentado como requisito para la obtención del título de Ingeniero en Nanotecnología.


**Autor:**

López Mera Cristhian Alexander

**Tutor:**

Ph. D. González Vázquez Gema

**Co-tutor:**

Ph. D. Briceño Sarah


Urcuquí, febrero 2023

# AUTORÍA

Yo, **CRISTHIAN ALEXANDER LÓPEZ MERA**, con cédula de identidad 1312705401 declaro que las ideas, juicios, valoraciones, interpretaciones, consultas bibliográficas, definiciones y conceptualizaciones expuestas en el presente trabajo; así cómo, los procedimientos y herramientas utilizadas en la investigación, son de absoluta responsabilidad de el/la autora (a) del trabajo de integración curricular. Así mismo, me acojo a los reglamentos internos de la Universidad de Investigación de Tecnología Experimental Yachay.

Urcuquí, febrero 2023.

Cristhian Alexander López Mera

CI: 1312705401

# AUTORIZACIÓN DE PUBLICACIÓN

Yo, **CRISTHIAN ALEXANDER LÓPEZ MERA**, con cédula de identidad 1312705401, cedo a la Universidad de Tecnología Experimental Yachay, los derechos de publicación de la presente obra, sin que deba haber un reconocimiento económico por este concepto. Declaro además que el texto del presente trabajo de titulación no podrá ser cedido a ninguna empresa editorial para su publicación u otros fines, sin contar previamente con la autorización escrita de la Universidad.

Asimismo, autorizo a la Universidad que realice la digitalización y publicación de este trabajo de integración curricular en el repositorio virtual, de conformidad a lo dispuesto en el Art. 144 de la Ley Orgánica de Educación Superior.

Urcuquí, febrero 2023.

Cristhian Alexander López Mera

CI: 1312705401

## Dedicatoria

*Quiero dedicar esta tesis a las personas más especiales en mi vida:*

*A mi mami y a mi papi, Nancy y Alex, porque este triunfo también es de ustedes. Es por ustedes que ahora soy quien soy, y eso es una huella indeleble que tendré por siempre en mi corazón.*

*A mis hermanos Ernesto y Marcelo, quienes me enseñaron lo que es tener, no uno, sino dos mejores amigos.*

*A mi novia Michu, quien me hizo saber que la felicidad la podía encontrar incluso sin estarla buscando.*

*A toda mi familia que en algún momento me brindaron su cariño y apoyo.*

*A mis gatas Negra y Manchitas, por pasar a mi lado largas tardes y noches de estudio.*

*A todo aquel que se tome un tiempito de leer esta tesis.*

Cristhian López Mera

## Acknowledgements

First of all, I would like to acknowledge my dad and my mom, Ángel and Nancy, for all the abnegation, advice, teachings, inspiration, and specially all the love and support they had given me since I was born. I have no doubt that without their effort, hard work and guidance, attaining this achievement would not be possible. I feel really blessed of having such that parents, who have raised me and my brothers in the terms of the true love. For showing me the actual meaning of the saying “the one who perseveres, reaches”. For these and an infinite of other reasons I am thankful with my parents, who have helped me to make this dream come true. To my brothers Ernesto and Marcelo, who have encouraged me and been an example of overcoming. To my girlfriend Michu, who has been my entire support during these last years. You have helped me to bring out the true scientist that was hide inside me. You made me believe in myself every time I felt that I could not get it. I’ve learnt a lot from you, and one of those things is the feeling of belonging: of being part of the Academia. For your every-day encouragement, I am truly thankful my love. To my advisor, professor Gema González for providing me the guidance that I really needed, for being patient to me and for teaching me (and all the School of Physical Science and Engineer) the characteristics of a leader. To my co-advisor, professor Sarah Briceño, who has taught me every single detail I know about the laboratory, for your patience, for your commitment and for your precious guidance. A special thanks to my professor Raúl Dávalos, to whom I owe all the effort invested for helping me to synthesize the first nanofibers at Yachay Tech University. Without your guidance, this would not be possible. Also, I would like to thank Professor Javier Álvarez, who helped me out to develop the biological assays. The time that we spent in the laboratory was a time in which I was able to learn a lot about another field of science that I love: the biology. To my alma máter, Yachay Tech University, institution that has provided me a top tier-high quality education. I will always be thankful for the formation received here. To my jurors, professor Floralba López and Professor Juan Lobos, who have dedicated me time for qualifying this work and making comments in order to improve the quality of this job. To my friends Nando, Carlos, Ricardo and Daniel, who have been a special a part of this journey called University. To the technicians of the Laboratory of the School of Physical Sciences and Engineering, Luis Corredor and Jonathan Escorza, who helped me a lot during the realization of this project. To my family, who somehow have inspired me to always looking forward and achieve my dreams. An special thanks to professor Werner Bramer and professor Julio Chacón, who were the ones that, with their amazing classes, could inspire me to take the way I am taking right now: being a scientist.

Cristhian López Mera

## Resumen

La técnica de electrohilado se considera una de las técnicas de fabricación de nanofibras más utilizadas y un método simple de bajo costo que puede lograr una producción en masa. Por un lado, se puede utilizar una amplia gama de polímeros como el polivinil alcohol (PVA) y el quitosano para fabricar nanofibras con fines biomédicos. Por otro lado, ha habido un especial interés en las propiedades biomédicas de las nanopartículas de óxido de cerio (ceria), sus efectos antiinflamatorios, resistencia al cáncer, angiogénesis y aplicaciones en ingeniería de tejidos. En este contexto, la fabricación de materiales nanoestructurados puede conducir al desarrollo de nuevos andamios biocompatibles funcionales. El presente trabajo tuvo como objetivo fabricar y estudiar nanofibras de PVA, quitosano y PVA/quitosano electrohiladas incrustadas con nanopartículas de ceria que pueden usarse como biomaterial antibacteriano y antifúngico. Se sintetizaron nanopartículas de ceria y luego se caracterizaron por el método UV/vis usando un espectrofotómetro estándar. Se prepararon soluciones poliméricas de 8% en peso de PVA, 4% en peso de quitosano y PVA/quitosano en diferentes proporciones de volumen y se doparon con nanopartículas de ceria. Las caracterizaciones estructurales y morfológicas de las nanofibras se llevaron a cabo utilizando espectroscopía de Raman, espectroscopía de rayos X de dispersión de energía (EDX), espectroscopía infrarroja transformada de Fourier (FTIR), análisis termogravimétrico y microscopía electrónica de barrido (SEM). Tanto la espectroscopía de Raman como la infrarroja mostraron picos característicos para las nanofibras de PVA y PVA/quitosano. El análisis termogravimétrico demostró que las nanofibras de PVA/quitosano poseían una mejor estabilidad térmica, comparadas con los polímeros individuales. Los análisis SEM y UV/vis confirmaron nanofibras que oscilaban entre 100 nm y 400 nm de diámetro. El análisis EDX mostró la presencia de nanopartículas de ceria en las nanofibras. Se realizaron ensayos antibacteriales y antifúngicos que demostraron inhibición bacteriana y fúngica por parte de las nanofibras de PVA dopadas con nanopartículas de óxido de cerio y las nanofibras de PVA/quitosano (70/30) dopadas con nanopartículas de óxido de cerio. En conclusión, se optimizaron parámetros para la fabricación de nanofibras puras y cargadas con nanopartículas de óxido de cerio de polímeros de PVA y PVA/quitosano; las nanofibras cargadas con nanopartículas de óxido de cerio mostraron un diámetro significativamente menor comparadas con las nanofibras puras de PVA y PVA/quitosano; las nanofibras de PVA y PVA/quitosano cargadas con nanopartículas de óxido de cerio mostraron inhibición bacteriana y fúngica.



**Palabras clave:** Nanofibras electrohiladas, polivinil alcohol, quitosano, nanoparticulas de óxido de cerio, propiedades antibacterianas.

## Abstract

The electrospinning technique is considered one of the most-commonly used nanofiber fabrication techniques and a simple low-cost method that can achieve scale-up mass production. On the one hand, a wide range of polymers, such as polyvinyl alcohol (PVA) and chitosan, can be used to manufacture nanofibers for biomedical purposes. On the other hand, there has been a special interest in the biomedical properties of cerium oxide (ceria) nanoparticles, its anti-inflammatory effects, cancer resistance, angiogenesis, and applications in tissue engineering. In this context, the fabrication of nanostructured materials can lead to the development of novel functioning biocompatible scaffolds. The present work aimed to fabricate and study electrospun PVA, chitosan, and PVA/ chitosan nanofibers embedded with ceria nanoparticles that can be used as an antibacterial and antifungal biomaterial. Ceria nanoparticles were synthesized and then characterized by UV/vis method using a standard spectrophotometer. 8% wt PVA, 4% wt chitosan, and PVA/chitosan polymeric solutions in different volume ratios were prepared and doped with ceria nanoparticles. Structural and morphological characterizations of the nanofibers were carried out by using Raman spectroscopy, Energy dispersive X-ray spectroscopy (EDX), Fourier transform infrared spectroscopy (FTIR), Thermo-gravimetric analysis (TGA) and scanning electron microscopy (SEM). Both FTIR and Raman spectroscopy analysis showed characteristic peaks for PVA and chitosan. TGA displayed that PVA/chitosan nanofibers presented a greater thermo-stability as compared with individual polymers. SEM analysis confirmed nanofibers ranging from 100 nm to 400 nm in diameter. EDX and UV/vis analysis demonstrated the presence of ceria nanoparticles in the nanofibers. Antibacterial and antifungal assays showed inhibition for both loaded ceria nanoparticles PVA nanofibers and loaded ceria nanoparticles PVA/chitosan (70/30) nanofibers. In conclusion, parameters were optimized for the fabrication pure and loaded ceria nanoparticles PVA and PVA/chitosan nanofibers; loaded ceria nanoparticles PVA and PVA/chitosan nanofibers showed a significant decrease in fiber diameter as compared to pure PVA and PVA/chitosan nanofibers; and loaded ceria nanoparticles PVA and PVA/chitosan nanofibers inhibited bacterial and fungal growth.



**Keywords:** Electrospun nanofibers, polyvinyl alcohol, chitosan, ceria nanoparticles, antibacterial properties.

# Contents

# List of Figures

# Chapter 1

# Introduction

The skin is the largest organ of the human body, playing a crucial role due to its functions, such as: homeostasis of fluids, protection against external biotics and abiotics factors, sensory detection, regulation of corporal temperature and self healing[1]. On the one hand, protecting the epidermis, which is the outermost layer of the skin and has high impermeability, helps to maintain healthy the inner organs of the body. On the other hand, loss or damage of the integrity of the skin may harm the skin functions, from lacerations to vasculature, damage of nerve bundles to even death[1]. For those reasons, the developing of tissue engineering is of relevant importance in order to treat moderate or severe injuries that can affect the skin.

Tissue engineering is a field of research that uses bioresorbable and biodegradable materials, which in conjunction with the use of scaffolds, have been proved to improve cell regeneration and cell growth[2]. Scaffolds are structures that serve as a support or matrix for materials of intrinsic interest and are designed to facilitate cellular growth and regeneration when implantation is required on a patient[3]. Scaffolds should have four main characteristics: i) biocompatibility, bioresorbable and controlled biodegradability; ii) highly interconnected-porous-three dimensional structures that allows cell growth and transport of nutrients and metabolic waste; iii) mechanical properties that match those of the of the tissue at implantation site and iv) a surface chemistry that promotes cell proliferation, attachment and differentiation[2]. Specifically, polymers (such as PVA and chitosan) can be designed into scaffolds for regenerative medicine and tissue engineering[4]. Over the last two decades, great advances in tissue engineering for wound healing have been merged due to a better understanding of cellular biology and cell-matrix scaffolding[5–7]. However, many factors like scarcity of implanting site and post-surgical scarring contributes to aesthetics concerns and partial loss of function of the skin in large skin damage[8]. Those are the reasons of why skin grafts and scaffolds are being used currently to correct and overcome skin injuries or post-surgical misaligned

defects of the repaired skin. In fact, it has been demonstrated that the use highly biocompatible polymeric scaffolds can enhance skin cell regeneration if used as a wound healing device[4]. In addition, nanostructured polymeric scaffolds such as collagen, alginate and chitosan have been used, effectively, to promote bone cell regeneration (osteogenesis)[4].

Both natural and synthetic polymers are used to mimic the anatomy and physiology of the skin. Dermal fibroblasts synthesize the collagen, that is responsible of interconnecting the extra-cellular matrix (ECM) of the dermis with the subcontinuous epidermis layer[5]. As collagen is the most abundant ECM protein, it is common that the earliest studies on wound healing tissue engineering focused on using collagen as a matrix[5]. Nowadays, a huge amount of polymers like collagen, chitosan, fibrin, hyaluronic acid, polyurethane, poly-lactic acid, poly-lactic glycol acid have been studied as matrix materials form dermal cell growth or dermal substitution[1,2,5,9,10]. Natural and synthetic polymers are used on electrospinning technique as well as blends of natural/synthetic polymers to fabricate nanofibers[11].

Electrospinning technique has emerged as a novel nanofiber fabrication technique, that can yield scale up mass production[12]. The technique consists in submitting a polymer solution flowing throw a needle under a stable electric filed so that the surface tension of the solution yield to the electric field, making it deposes on a collector plate[12]. This process allows the formation of fibers in the micron or nano scale, that can be used as a scaffold for tissue engineering[2]. Electrospinning technique is so versatile that several variables can be controlled, such as voltage applied, distance from the tip to the collector, flow rate and diameter of the needle. For its novelty, ease learning and control of parameters, this techniques is one of the most used for the development of nanofibers in the field of synthetic biology, biomedicine and nanomedicine[12].

Also, cerium oxide (ceria) nanoparticles have shown promising therapeutic, diagnosis, antibacterial, antifungal and anticancer properties[13–17].In fact, ceria nanoparticles have played an essential role in regenerative medicine and tissue engineering, specially for theragnostic and bioimaging purposes; this is mainly due to its oxidant resistance (antioxidant activity)[16]. This properties makes ceria nanoparticles the perfect candidate to be embedded into polymeric matrices to enhance their properties as scaffolds used for tissue engineering, making this complexes biomaterials a potential skin graft and drug delivery systems[18].

In a study done by Motasadizadeh, *et al.* (2022)[19], the authors developed electrospun poly(vinyl alcohol)/chitosan-g-poly(N-vinyl imidazole) (PVA/CS-g-PNVIM) containing titanium dioxide/curcumin (CUR) with several biomedical properties, such as controlled drug release, wound healing and closure,

antibacterial and antifungal activity. In their research, mechanical and structural properties of the biomaterial synthesized were measured using Fourier transform infrared spectroscopy, X-ray diffraction, scanning electron microscopy and tensile testing. Biological properties were investigated using degradation studies, drug release, and antibacterial in-vitro and in-vivo tests. With this work, the authors could conclude that the nanofibers are promising for biocompatible antibacterial wound dressing applications. Additionally, Shenata, *et al.* (2016), presented a research in which they synthesized fluorescent PVA electrospun nanofibers doped with ceria nanoparticles, obtaining good results for application in the bioimaging and environmental monitoring fields. These researches, and over a thousand more, demonstrates that the developing of polymeric scaffolds doped with lanthanide elements, such as cerium, is of greatest impact for tissue engineering nowadays.

## 1.1 Problem Statement

The development of novel biomaterials that can be used as scaffolds is of attractive attention in the tissue engineering research field. Among them, nanofibers are scaffold materials that can serve as carriers for several compounds (nanoparticles, drugs, hydroxyapatite, etc) to be deliberated in a controlled way due to its quenching capacity and nanoporous structures. Specifically, chitosan is a super biocompatible material that possess intrinsic biological properties, such as inhibition of bacteria and fungus [20].

The synthesis of ceria nanoparticles doped nanofibers provides extra characteristics [14] to their structures and is relevant in order to create materials that can mimic certain functionalities of the human body. A wide number of publications using polymeric scaffolds have been considered as novel for the huge range of applications that this type of structures have [4]. In this context, the fabrication of new polymeric scaffolds is of great importance for the advancement and development of more intelligent materials that adapt to human needs. For the previous explained reasons, this project proposes using synthetic polymers such as PVA and natural polymers such as chitosan to develop electrospun nanofibers and doping them with cerium oxide nanoparticles; with the aim of studying its antibacterial and antifungal properties. All this, taking into account the numerous research done on electrospinning of polymeric scaffolds doped with metallic nanoparticles.

## 1.2 General and Specific Objectives

### 1.2.1 General Objetive

1. To synthesize electrospun PVA and chitosan nanofibers with embedded ceria nanoparticles that can be used as a antibacterial or antifungal biomaterial.

### 1.2.2 Specific Objectives

1. To synthesize PVA and chitosan polymeric solutions.
2. To synthesize and characterize ceria nanoparticles.
3. To dope PVA and chitosan polymeric solutions with ceria nanoparticles.
4. To fabricate electrospun nanofibers with embedded ceria nanoparticles and characterize them.
5. To make a complete physical-chemical characterization of the synthesized nanofibers.
6. To make a preliminary antibacterial and antifungal susceptibility tests on the synthesized nanofibers.

# Chapter 2

# Theoretical Background

## 2.1 Nanotechnology

In the simplest possible way, nanotechnology can be defined as technology at the nanoscale[21].Various definitions of the components of the nanotechnology, such as nanoparticles, also refer to the nanoscale. The definition of nanotechnology is incomplete in the absence of the definition of nanoscale. The nanoscale comprises the range from 1 nm to 100 nm. With those definitions clearly stated, nanotechnology can be defined in a proper manner. Then, SCENIHR dictionary definition of nanotechnology is "the design, characterization, production and application of materials, devices and systems by controlling the shape and size in the nanoscale"[21]. The emphasis in controlling size is really important because nanotechnology focuses on the interactions that take place on the potential energy surface of the atoms and molecules considered, and that distinguishes it from Chemistry. Hence, nanotechnology can be finally defined as the engineering of materials and devices structured at the nanoscale with processes capable of manipulating individual atoms or nanoblocks with ultra-precision resulting in systems with fundamental new properties and functions[21]

### 2.1.1 Nanoparticles

Nanoparticles can be defined as a dispersion or particles with a size ranging from 10 to 1000 nm. The term nanoparticles also includes the terms nanospheres and nanocapsules, and the formation of these systems depends on the method of preparation[22]. In general, nanoparticles are used as drug delivery systems due to its larger surface area and its capacity to enter the extracellular matrix[23]. The advantages of using nanoparticles as drug delivery systems are: (i) surface characteristics can be controlled;(ii) release of drugs and localization during transportation can be controlled; (iii) specific targeting can be achieved; (iv)

various routes of administration can be used[22]. Another application of nanoparticles are in biology and medicine as they are used for imaging, cell labelling and theranostic applications[24]; in tissue engineering as they are used as scaffolds in order to mimic certains functionalities of human body[25].

### 2.1.2 Ceria nanoparticles

Cerium is among the 17 rare earth elements or lanthanides and is the most abundant of this[26]. Cerium can exist in both 3+ and 4+ elements, therefore, it found as $CeO_2$ and $Ce_2O_3$ in the bulk state. In the past few years, the importance of ceria nanoparticles in biomedical applications is growing, and due to its dual oxidation state ceria is considered as an ideal catalyst[26,27]. Ceria nanoparticles ($CeO_2$-NPs) are nanocrystalline derived from cerium[26,27]. Although, the nanoparticles of ceria have been studied since the early 1970s, it is only in recent years that thanks to the use of better synthesis methods and sophisticated techniques that has been possible to characterize structural and electronic properties[26,27]. Images of ceria nanoparticles obtained by high-resolution transmission electron microscopy (HRTEM) indicated that in the size range 3 – 10 nm. the particles are crystalline, and their shape predominantly corresponds to truncated octahedra[26,27].

## 2.2 Polymers

### 2.2.1 Chitosan

Chitosan, a non-toxic natural biopolymer[28] derived from the deacetylation of chitin[28 29], is a family of linear polysaccharides[30] composed of variable amounts of linked residues (1→4) of N-acetyl -2-amino-2-deoxy-D-glucose (glucosamine, GlcN) and 2-amino -2-deoxy-D-glucose (N-acetyl-glucosamine, GlcNAc)[29]. Chitosan is soluble in aqueous media[31], slightly acidic[20], so it has a variety of applications ranging from solutions, gels, fibers[31] , biopharmaceutical products[30], among others. Furthermore, chitosan being a cationic polymer[32] (unique in nature[29]) forms effective non-viral gene delivery complexes, due to its interaction with polyanionic nucleic acids[30]. Its charge density depends on the degree of acetylation and pH of the medium, and its solubility depends on the degree of acetylation, molecular weight, ionic concentration, pH, temperature, nature of the acid used for protonation, the distribution of acetyl groups in the chain, conditions of isolation and drying of the polysaccharide[31]. The structural formula of chitosan is shown in figure 2.1 and its chemical formula is (C6H11O4N)n[20].

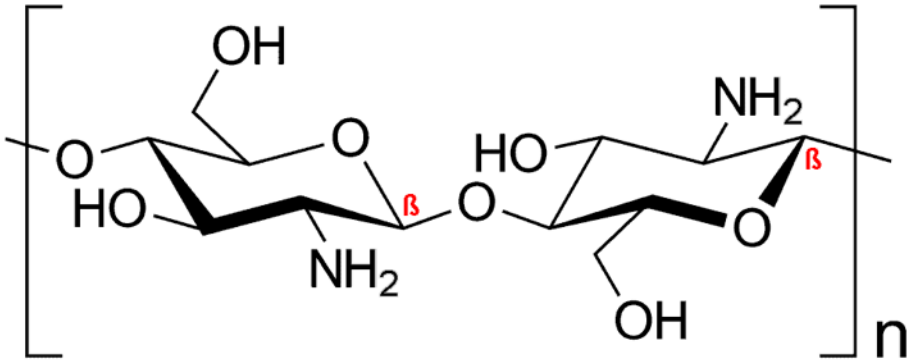


Figure 2.1: Structural formula of Chitosan. Retrieved from[33]

### 2.2.2 Polyvinyl Alcohol (PVA)

Polyvinyl alcohol (PVA) is a linear synthetic polymer produced via partial or full hydrolysis of polyvinyl acetate to remove the acetate groups[34]. The amount of hydroxylation determines the physical characteristics, chemical properties, and mechanical properties of the PVA[34]. The resulting PVA polymer is highly soluble in water but resistant to most organic solvents. The greater the degree of hydroxylation and polymerization of PVA, the lower its solubility in water and the more difficult it is to crystallize[34].

## 2.3 Electrospinning

Electrospinning was first observed in 1987, then studied in detail by Zeleny in 1914[35], and finally patented by Formhals in 1934[36]. The process of electrospinning offers exclusive conditions for producing nanofibers with controlled size and porosity[37]. Unlike typical mechanical fiber-spinning technique, the electrospinning process provides the tools and versatility to spin a wide variety of polymeric fibers in the nanometric scale. Also, electrospun nanofibers have the characteristic of having smaller pores and a higher surface area in comparison with regular fibers[38]. The process of electrospinning has gained attention in the last decades because of its interaction with different research fields, such as pharmaceutical, biomedical, tissue engineering scaffolds, filtration, and others[12].

There exist several particulars that make electrospinning technique one of the most reliable ones to create nanofibers. For this reason, in this section, the most important aspects related to electrospinning technique are going to be treated in detail, including the technique itself, the set of controllable parameters of the technique, the most used polymers for electrospinning, nanofibers, and finally, the applications of the

electrospun nanofibers.

### 2.3.1 Technique of electrospinning

Electrospinning is a technique used for the formation of polymer fibers that employs electrical forces to produce fibers ranging in diameter from 2 nm to several micrometers. Both natural and synthetic polymers are used in order to produce nanofibers[12]. In electrospinning technique a DC voltage in the range of several kV is required to generate the sufficient electrostatic force to break down surface tension of polymers used. This technique is based on the principle that weaker forces of surface tension in the charged polymer are overcame by strong electrical repulsive forces produced by the power suppl[39]. In Figure 2.2 is depicted a schematic of the electrospinning technique, where all the parts that made up the apparatus are shown. There are two standard set up for electrospinning apparatus: vertical and horizontal. Also electrospinning is performed at room temperature and at normal atmospheric conditions[40]. Electrospinning system consists of three main components: a high voltage power supply, a spinneret and a grounded collecting plate (that usually is a metal fixed plate or a rotating cylinder). The electrospinning technique uses a high voltage source to inject charge of certain polarity into the polymer located at the spinneret mechanism and then, the solution is accelerated towards the collector that is also connected to the voltage source and has an opposite polarity[41].

## 2.4 Characterization Techniques

### 2.4.1 Scanning electron microscopy (SEM)

The scanning electron microscope (SEM) is considered one of the most versatile instruments to examinate and analyses the microstructure morphology and chemical composition characterizations[42,43]. SEM is an electron microscope that utilizes the interaction between the focused beam of electrons with the sample to generate a topological image and relative composition. The focused beam of electron upon contact with the sample will produce secondary electrons (SEs), back scattered electrons (BSE), and characteristic X-ray, which are detected and displayed on monitor. The main components in a typical SEM include electron source, column with electromagnetic lenses, electron detector, sample chamber, and the computer display[43,44]. As mentioned above, the formation of SEM image is mainly correlated with the detection of signals that receive from the interactions between electron signals and the scanned samples. In general, there are two type of interactions that occur, called elastic and inelastic interactions. In the inelastic interaction occur that low energy of secondary electrons is emitted from the samples after bombarded by the primary beam electrons. This interaction is characterized by negligible energy loss during the

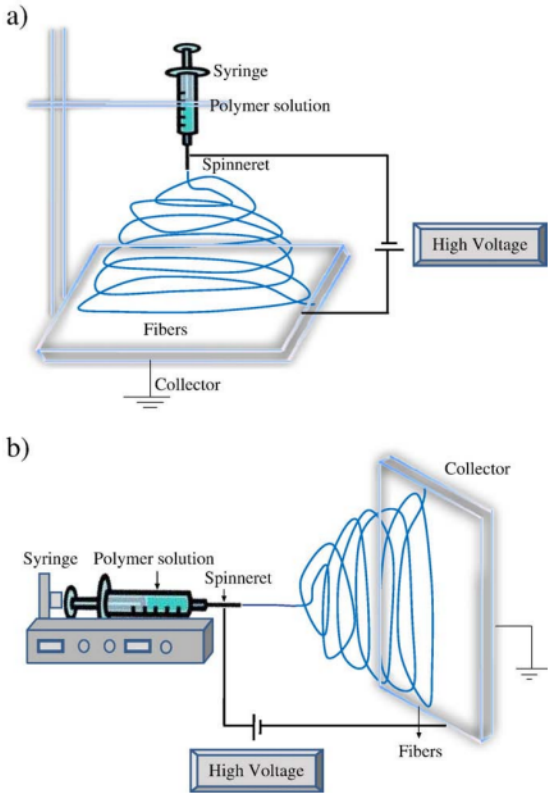


**Fig. 1.** Schematic diagram of set up of electrospinning apparatus (a) typical vertical set up and (b) horizontal set up of electrospinning apparatus.

Figure 2.2: Schematic of Electrospinning apparatus and technique. Part (a) describes the model for a vertical set up and part (b) describes the horizontal set up[12].

| Polymers | Applications | Characterizations |
|---|---|---|
| Poly(glycolide) (PGA) | Nonwoven TE[a] scaffolds | SEM[b], TEM[c], *in vitro* rat cardiac fibroblast culture, *in vivo* rat model |
| Poly(lactide-co-glycolide)(PLGA) | Biomedical applications, wound healing | SEM, WAXD[d], SAXS[e], degradation analysis |
| Poly(ε-caprolactone) (PCL) | Bone tissue engineering | SEM, *in vitro* rat mesenchymal stem cell culture |
| Poly(l-lactide) (PLLA) | 3D cell substrate | SEM, *in vitro* human chondrocyte culture |
| Polyurethane (PU) | Nonwoven tissue template wound healing | SEM, *in vivo* guinea pig model |
| Poly(ethylene-co-vinyl alcohol) (PEVA) | Nonwoven tissue engineering scaffold | SEM, *in vitro* human aortic smooth muscle cell and dermal fibroblast cultures |
| Polystyrene (PS) | Skin tissue engineering | SEM, *in vitro* human fibroblast, keratinocyte, and endothelial single or cocultures |
| Syndiotactic 1,2-polybutadiene | Tissue engineering applications | ESEM[f], XRD[g], FTIR[h] |
| Fibrinogen | Wound healing | SEM,TEM,mechanical Evaluation |
| Poly (vinyl alcohal)/cellulose acetate (PVA/CA) | Biomaterials | SEM, FTIR, WAXD, mechanical evaluation |
| Cellulose acetate | Adsorptive membranes/felts | SEM, FTIR |
| Poly(vinyl alcohol) | Wound dressings | SEM, EDX[i] |
| Silk fibroin, silk/PEO[j] | Nanofibrous TE scaffold | SEM, FTIR, XPS[k] |
| Silk | Biomedical Applications | SEM, TEM, WAXD |
| Silk fibroin | Nanofibrous scaffolds for wound healing | SEM, ATR-IR[l], $^{13}$C CP/MAS NMR, WAXD, NMR[m], *in vitro* human keratinocyte culture |
| Silk/chitosan | Wound dressings | SEM, viscosity analysis, conductivity measurement |
| Chitosan/PEO | TE scaffold, drug delivery, wound healing | SEM, XPS, FTIR, DSC[n] |
| Gelatin | Scaffold for wound healing | SEM, mechanical evaluation |
| Hyaluronic acid, (HA) | Medical implant | SEM |
| Cellulose | Affinity membrane | SEM, DSC, ATR-FTIR[o] |
| Gelatin/polyaniline | Tissue engineering scaffolds | SEM, DSC, conductivity measurement, tensile testing |
| Collagen/chitosan | Biomaterials | SEM, FTIR |

Figure 2.3: Natural and synthetic polymers used in electrospinning, its applications and most common characterization techniques for each one. Adapted from reference [12].

collision and a wide-angle directional change of the scattered electron. Instead, elastic interaction consists to the deflection of primary electron upon contact with the sample atomic nucleus (or electrons of similar energy). The deflection of the scattered electrons is at angle of more than 90 degrees are called back scattered electrons (BSE) and can be utilized for sample imaging[43].

### 2.4.2 Fourier transform infrared spectroscopy (FTIR)

The Fourier Transform is a mathematical tool which purpose is to decompose a complex wave form (that is not sinusoidal) into a sum of sinusoids. It is told that if the sum of sinusoids is equal to the original wave, the Fourier transform a waveform has been reached[45]. In Figure 1 can be seen an schematic of how the Fourier transform of a waveform is interpreted. In this context, the Fourier transform can operate on several functions that works in the space or time domains and transform them into functions which works on the spatial frequency or temporal frequency domain[46]. In order to do that, a series of calculation must be developed to achieve the Fourier Integral (equation 2.1).

$$H(f) = \int_{-\infty}^{\infty} h(t)e^{-j2\pi ft}dt \tag{2.1}$$

The Fourier Integral is a complex operator that transforms a function $h(t)$ which is variable in time, into a function $H(f)$ which is variable in frequency[45].

From the Fourier integral it comes the Fast Fourier Transform (FFT), that is a computational algorithm developed to reduce the computing time of the discrete Fourier transform to a time that is proportional to N$log_2$N and has become into a problem solving tool in the research, educational, computational,biomedical and military fields[45].

The vibrational properties of functional groups and cofactors are really sensitive to minimum structural changes and can be associated with characteristic absorption bands that tell us the nature of its fundamental vibrations[47]. Fourier Transform Infrared Spectroscopy probes that molecular vibrations by using infrared light. In specific FTIR detect the asymmetrical vibration of all molecules (including aminoacids and water that are hard to measure with other spectroscopy techniques)[47]. The stretching vibrations of the functional groups present in molecules can be modeled with an harmonic oscillator as the bonding between two atoms can be represented by two point masses separated by a spring[47]. Under this model, the bond strength is analogous to the $k$, the spring tenseness, $m_1$ and $m_2$ are the corresponding masses of the atoms that form the bonding[47]. Thus, the frequency of vibration of the functional groups can be expressed by $v$ in equation 2.2

$$v = (1/2\pi c)\sqrt{(k\,(m_1 + m_2)\,/m_1 m_2)} \tag{2.2}$$

Where triple or double bonds will have a higher frequency of oscillation as compared with single bonds[47]. This effect is explained at detail in figure 2.

In a FTIR spectrum (see figure 4), different absorption peaks that are related to the intensity of vibration of functional groups can be observed. The position of the IR absorption peaks (see figure 3) of a sample measured by FTIR spectroscopy will depend specifically on the functional groups present on the molecules of the sample[48]. In the research done by[49], aminoacids (C-O) peaks are shown at 1100 $cm^{-1}$, hydroxy groups (O-H) between 3100-3350 $cm^{-1}$, ethers (C-H) at 2900 $cm^{-1}$, carbonyl groups (C=O) between 1730 and 3100 $cm^{-1}$, carboxylic acid groups(OH and C=O) at 2900 $cm^{-1}$, amine groups (N-H) at 3200 $cm^{-1}$ and nitrile groups (C=N) at 2250 $cm^{-1}$.

# Chapter 3

# Methodology

## 3.1 Reagents and Apparatus

Polyvinyl alcohol (PVA) (average Mw 130,000, 99+% hydrolized), chitosan (CS) (high molecular weight, $H_2O$ insoluble), ammonium hydroxide ($NH_3OH$)(+99% reagent grade), cerium Sulfate (III) ($CeSO_4$) (reagent grade 99+%) and acetic acid (+99% reagent grade) were purchased from Aldrich and Sigma Co LLC. A heating/stirring plate (HORIBA) was used for the preparation of polymeric solutions. Electrospinning $Spraybase^{TM}$ was utilized at different working conditions for producing nanofibers. A standard spectrophotometer (Thermo Scientific), an FTIR (Thermo Scientifc), a Ramman spectrometer (HORIBA), and a Scanning electron microscope ($PHENOMPROX$) (see figure3.1) were used to perform the respective characterization of both synthesized nanofibers complexes and ceria nanoparticles. An incubator and agitator (Thermo Scientific) were used for the preparation of culture medium and grwoth of bacteria and fungi for biological tests.

## 3.2 Synthesis Methods

In this work, ceria nanoparticles, PVA, and chitosan polymers have been synthesized. A polymeric complex of PVA and chitosan have been synthesized, as well as the corresponding ceria nanoparticles doping of every polymeric solutions. A posterior electrospinning of fibers was carried out by using pure and doped polymeric systems.

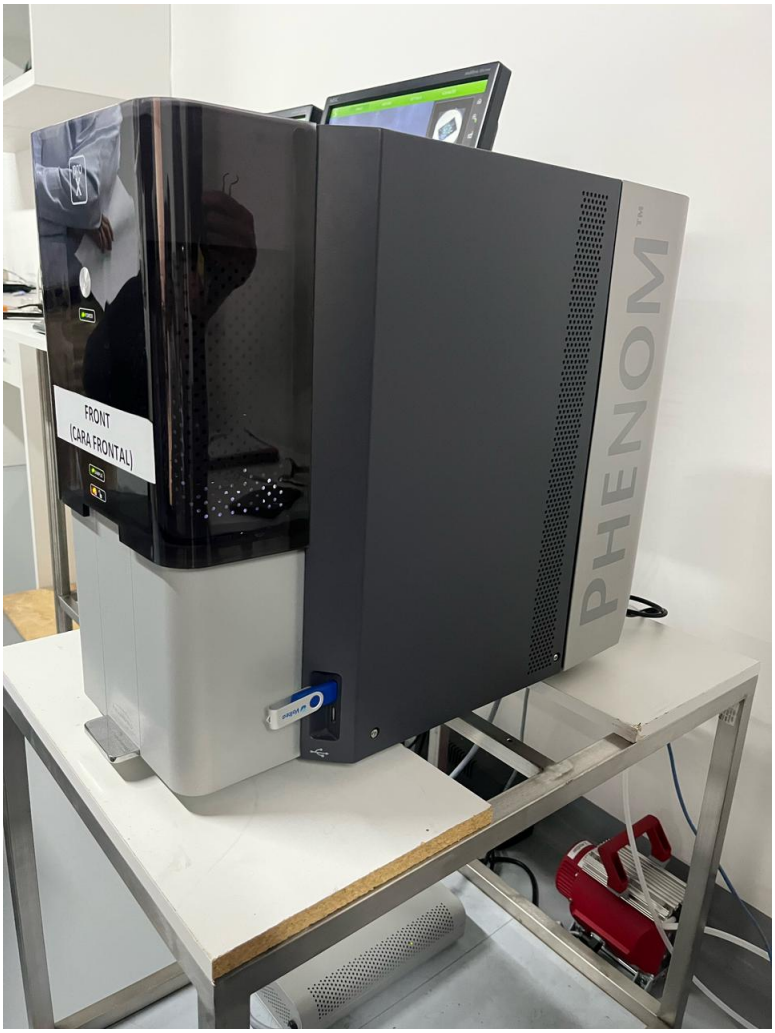


Figure 3.1: Scanning electron microscope used for measurements of doped and undoped polymeric nanofibers.

### 3.2.1 Ceria Nanoparticles

A 0.05 M solution of cerium sulfate was prepared by diluting 0.16 g of cerium sulfate in 10 mL of double distilled water at a temperature of 60 °C and constant stirring of 800 rpm. Simultaneously, 10 mL of ammonium hydroxide (25%) was added to 142 mL of double distilled water to form a 0.5 M $NH_4OH$ solution. Cerium sulfate solution was held at a constant temperature and stirring as before, and 25 mL of ammonium hydroxide solution was added drop-wise until a yellowish precipitate started to form. The solution containing ceria nanoparticles was sonicated using a power of 60%, and a working time of 30 minutes with pulses of 6.0 seconds each 7.0 seconds to disperse ceria nanoparticles. Colloidal ceria nanoparticles were characterized and stored for their further use.

### 3.2.2 Synthesis of PVA polymeric solution

Three PVA stock solutions were prepared. 4.0; 6.0 and 8.0 g of PVA flakes were added to 100 mL of distilled water at 80 °C and stirred at 1000 rpm for 6 hours to obtain 4%, 6%, and 8% homogeneous PVA stock solutions, respectively. The stock solutions were kept at room temperature and constant stirring of 600 rpm overnight to promote an enhanced hydrolyzation of the polymer. After 24 hours, the stock solutions were centrifuged at 12000 g for 15 minutes to make any lump formation precipitate. The stock solutions were decanted and stored for further use.

### 3.2.3 Synthesis of Chitosan polymeric solution

On the other hand, three chitosan (CS) stock solutions were prepared. A solution of acetic acid (10%) (v/v) was used as solvent for chitosan. 2.0, 3.0, and 4.0 g of high molecular weight chitosan were added to 100 mL of acetic acid 10% (v/v) at 60 °C and stirred at 1200 rpm for 8 hours to obtain 2%, 3%, and 4% homogeneous chitosan stock solutions, respectively. The stock solutions were covered by a watch glass and left at 40 °C and constant stirring of 800 rpm overnight to promote an enhanced hydrolyzation of chitosan. After 24 hours, the stock solutions were centrifuged at 15000 g for 30 minutes to make any lump formation precipitate. The stock solutions were decanted and stored for further use.

### 3.2.4 Synthesis of PVA/ Chitosan polymeric complex solution

Three PVA/chitosan polymeric complexes were prepared. 8% (wt) PVA solution and 4% (wt) CS solution were chosen to make the polymeric complexes. PVA and CS solutions were mixed to prepare PVA/CS complex solutions in different volume ratios: 30/70, 50/50, and 30/70. PVA/CS solutions were put in a

heating/stirring plate at 40 °C and 600 rpm for 1 hour to perform a proper mixture of polymers. PVA/CS complex solutions were stored for further ceria nanoparticle doping.

### 3.2.5 Doping of PVA, chitosan, and PVA/Chitosan polymeric solutions with ceria nanoparticles

PVA, chitosan, and PVA/chitosan polymeric solutions were doped with different volumetric concentrations of ceria nanoparticles. Stock solutions used were 8% wt PVA, 4% wt CS, and PVA/CS (volume ratios of 70/30,50/50 and 30/70 ). 5, 10, and 15 mL of colloidal solution of ceria nanoparticles were mixed with each stock solution to form doped ceria nanoparticles polymeric complexes with different ceria nanoparticles concentration. Doped ceria nanoparticles polymeric solutions were held at 50 °C and constant stirring of 800 rpm to evaporate the exceeding solvent, keep the initial polymer concentration, and disperse the nanoparticles. Sonication treatment with a power of 60% and pulses of 6.0 seconds every 7.0 seconds for 45 minutes was applied to every doped ceria nanoparticles polymeric solution to perform a better dispersion of nanoparticles. Doped ceria nanoparticles polymeric solutions were safely stored for their respective electrospinning treatment.

### 3.2.6 Electrospinning of PVA, CS and PVA/CS fibers

Electrospinning equipment $SprayBase^{TM}$ was used to fabricate the nanofibers. Pure synthesized and doped ceria nanoparticles PVA, CS, and PVA/CS polymers were used for the fabrication of nanofibers. Working conditions of the electrospinning machine: voltage applied, needle diameter, polymer flow rate, volume of sample, distance between needle and collector, temperature and humidity of the room were also recorded. Electrospun samples were collected in a stainless steel collector plate (Figure 3.2) covered by aluminum foil. Fibrous-mat samples were coded for a better organization of the data obtained. The most effective volume ratio of PVA/CS was (70/30), based on initial composition of polymeric solution, and only this one was used to produce PVA/CS (70/30) nanofibers.

## 3.3 Characterization Methods

### 3.3.1 UV/vis spectroscopy

UV/vis spectroscopy of synthesized ceria nanoparticles was done with a HORIBA spectrophotometer. A 10 uL micropipette was used to deposit a drop of solution containing ceria nanoparticles in the sample holder of the spectrophotometer. Measurements of absorbance were performed every 1 nanometer in an

Figure 3.2: Stainless steel collector plate used to recollect electrospun nanofibers

encompassed range from 200 to 800 nm. The expecting absorbance peak is located between 280 and 315 nm.

### 3.3.2 Fourier transform infrared spectroscopy

The FTIR spectra was taken using the AGILENT Cary-630 Fourier transform infrared spectrometer, which belongs to Yachay Tech University and is located in the laboratory of sample preparation of the School of Biological Sciences and Engineering.

### 3.3.3 Raman spectroscopy

A Raman spectroscopy analysis was conducted on PVA, PVA/chitosan (70/30), doped ceria nanoparticles PVA and doped ceria nanoparticles PVA/chitosan (70/30) nanofibers. A 532 nm laser was used with a power of 50%. Acquiriing time was set to 20 seconds with 5 five accumulations per measurement. Range of Raman wavenumber was set between 20 and 3500 $cm^{-1}$. A x100 objective was used for microscopy of the nanofibers. Grating of the instrument was set to 600. To check for homogeneity of the nanofiber samples, each sample was measured 4 times at 4 different points.

### 3.3.4 Scanning electron microscopy (SEM) and Energy-dispersive X-ray spectroscopy (EDX)

Microstructural analysis was carried out in a *PhenomProX* scanning electron microscope with a coupled EDX spectroscopy sensor. The distance from the electron source to the sample was a fixed value from this model to look for a better resolution. The maximum possible resolution of the SEM was 10 nm. The acceleration voltage used was 10 kV. Samples of electrospun fibers were stuck to an SEM sample holder coated with graphite tape. Graphite tape is a conductor material that allows electrons to interact with the sample. After that, the samples were washed out with compressed air to reach a uniform thickness of the fibrous mat within the sample holder. The EDX detector allowed us to know the composition of the sample. An EDX point analysis was carried out both in doped ceria nanoparticles PVA and PVA/chitosan (70/30) nanofibers with an applied voltage of 15 kV. Five points, located in parts with different contrast, were measured in both samples.

## 3.4 Biological tests

### 3.4.1 Anti-bacterial susceptibility test

Luberia broth (LB) agar solid culture media was prepared according to the method proposed by Liu[50], and then kept in the refrigerator at 4 °C until its further use. Simultaneously, 20 mL of LB liquid medium was prepared and put on a test tube. Immediately, 1 mL of *Escherichia coli ATCC 25922* pre-culture was inoculated on the LB liquid medium and grown at 37 °C with constant agitation of 230 rpm for 3 hours. A dilution 1/10 was performed on *E.coli* cultured cells, for a proper measurement of concentration. A nanodrop was used to measure the concentration of bacteria cells grown (Program OD600) at 600 nm. Measurements on Nanodrop were done 5 times and the average value taken for the estimation of the actual cell concentration by using 3.3. While calculations of concentration were performed, LB solid medium was left under UV light for 15 minutes for a proper sterilization. After calculations, a total concentration of $10^8$ cells/ mL was laid on prepared LB solid medium. Square samples of 4 mm per side of doped ceria nanoparticles PVA nanofibers and doped ceria nanoparticles PVA/chitosan (70/30) nanofibers were placed at the plate as treatments. Nourseothricin (240$\mu$g/mL) was used as positive control, acetic acid and bare PVA nanofibers were used as negative controls. The plate with the cells, controls and treatments were left in an incubator at 37 °C for 24 hours.

### 3.4.2 Antifungal susceptibility test

Yeast peptone dextrose (YPD) agar solid culture medium was prepared according to the method proposed by Liu[51], and then kept in the refrigerator at 4 °C until its further use. Simultaneously, 20 mL of YPD liquid medium was prepared and put on a test tube. Immediately, 1 mL of *Candida albicans* pre-culture was inoculated on the YPD liquid medium and grown at 37 °C with constant agitation of 210 rpm for 1.5 hours. A dilution 1/20 was performed on *Candidaalbicans* cultured cells, for a proper measurement of concentration. A nanodrop was used to measure the concentration of bacteria cells grown (Program OD600) at 600 nm. Measurements on Nanodrop were done 5 times and the average value taken for the estimation of the actual cell concentration by using 3.3. While calculations of concentration were performed, YPD solid medium was left under UV light for 15 minutes for a proper sterilization. After calculations, a total concentration of $10^8$ cells/ ml was laid on prepared YPD solid medium. Square samples of 4 mm per side of doped ceria nanoparticles PVA nanofibers and doped ceria nanoparticles PVA/chitosan (70/30) nanofibers were placed at the plate as treatments. Fluconazole (25$\mu$g/mL) was used as positive control, acetic acid and bare PVA nanofibers were used as negative controls. The plate with the cells, controls and treatments were left in an incubator at 37 °C for 24 hours.

Absorbance at 660nm. Number of cells x $10^7$/ml

| Abs | cells/ml | Abs | cells/ml | Abs | cells/ml | Abs | cells/ml |
|---|---|---|---|---|---|---|---|
| 0 | 0 | 0.38 | 1.627 | 0.76 | 3.281 | 1.14 | 4.935 |
| 0.01 | 0.017 | 0.39 | 1.671 | 0.77 | 3.324 | 1.15 | 4.978 |
| 0.02 | 0.06 | 0.4 | 1.714 | 0.78 | 3.368 | 1.16 | 5.022 |
| 0.03 | 0.104 | 0.41 | 1.758 | 0.79 | 3.411 | 1.17 | 5.065 |
| 0.04 | 0.147 | 0.42 | 1.801 | 0.8 | 3.455 | 1.18 | 5.109 |
| 0.05 | 0.191 | 0.43 | 1.845 | 0.81 | 3.499 | 1.19 | 5.152 |
| 0.06 | 0.234 | 0.44 | 1.888 | 0.82 | 3.542 | 1.2 | 5.196 |
| 0.07 | 0.278 | 0.45 | 1.932 | 0.83 | 3.586 | 1.21 | 5.239 |
| 0.08 | 0.321 | 0.46 | 1.975 | 0.84 | 3.629 | 1.22 | 5.283 |
| 0.09 | 0.365 | 0.47 | 2.019 | 0.85 | 3.673 | 1.23 | 5.326 |
| 0.1 | 0.409 | 0.48 | 2.062 | 0.86 | 3.716 | 1.24 | 5.370 |
| 0.11 | 0.452 | 0.49 | 2.106 | 0.87 | 3.760 | 1.25 | 5.413 |
| 0.12 | 0.496 | 0.5 | 2.149 | 0.88 | 3.803 | 1.26 | 5.457 |
| 0.13 | 0.539 | 0.51 | 2.193 | 0.89 | 3.847 | 1.27 | 5.500 |
| 0.14 | 0.583 | 0.52 | 2.236 | 0.9 | 3.890 | 1.28 | 5.544 |
| 0.15 | 0.626 | 0.53 | 2.280 | 0.91 | 3.934 | 1.29 | 5.588 |
| 0.16 | 0.670 | 0.54 | 2.323 | 0.92 | 3.977 | 1.3 | 5.631 |
| 0.17 | 0.713 | 0.55 | 2.367 | 0.93 | 4.021 | 1.31 | 5.675 |
| 0.18 | 0.757 | 0.56 | 2.410 | 0.94 | 4.064 | 1.32 | 5.718 |
| 0.19 | 0.800 | 0.57 | 2.454 | 0.95 | 4.108 | 1.33 | 5.762 |
| 0.2 | 0.844 | 0.58 | 2.498 | 0.96 | 4.151 | 1.34 | 5.805 |
| 0.21 | 0.887 | 0.59 | 2.541 | 0.97 | 4.195 | 1.35 | 5.849 |
| 0.22 | 0.931 | 0.6 | 2.585 | 0.98 | 4.238 | 1.36 | 5.892 |
| 0.23 | 0.974 | 0.61 | 2.628 | 0.99 | 4.282 | 1.37 | 5.936 |
| 0.24 | 1.018 | 0.62 | 2.672 | 1 | 4.325 | 1.38 | 5.979 |
| 0.25 | 1.061 | 0.63 | 2.715 | 1.01 | 4.369 | 1.39 | 6.023 |
| 0.26 | 1.105 | 0.64 | 2.759 | 1.02 | 4.412 | 1.4 | 6.066 |
| 0.27 | 1.148 | 0.65 | 2.802 | 1.03 | 4.456 | 1.41 | 6.110 |
| 0.28 | 1.192 | 0.66 | 2.846 | 1.04 | 4.499 | 1.42 | 6.153 |
| 0.29 | 1.235 | 0.67 | 2.889 | 1.05 | 4.543 | 1.43 | 6.197 |
| 0.3 | 1.279 | 0.68 | 2.933 | 1.06 | 4.587 | 1.44 | 6.240 |
| 0.31 | 1.322 | 0.69 | 2.976 | 1.07 | 4.630 | 1.45 | 6.284 |
| 0.32 | 1.366 | 0.7 | 3.020 | 1.08 | 4.674 | 1.46 | 6.327 |
| 0.33 | 1.409 | 0.71 | 3.063 | 1.09 | 4.717 | 1.47 | 6.371 |
| 0.34 | 1.453 | 0.72 | 3.107 | 1.1 | 4.761 | 1.48 | 6.414 |
| 0.35 | 1.497 | 0.73 | 3.150 | 1.11 | 4.804 | 1.49 | 6.458 |
| 0.36 | 1.540 | 0.74 | 3.194 | 1.12 | 4.848 | 1.5 | 6.501 |
| 0.37 | 1.584 | 0.75 | 3.237 | 1.13 | 4.891 | | |

Figure 3.3: Table with values of absorbance for program OD600 of Horiba Nanodrop, for calculation of the concentration of cultured cells in cells/ml. Values developed by professor Javier Alvarez Botas (School of Biological Sciences and Engineering).

# Chapter 4

# Results & Discussion

## 4.1 Structural and morphological characterization

### 4.1.1 UV/vis spectroscopy

In Figure 4.1 can be seen the UV/vis absorbance spectrum measured for $CeO_2$ synthesized nanoparticles. A strong, well- defined and sharp absorbance peak at 312 nm can be appreciated. Synthesized $CeO_2$ nanoparticles exhibited a strong absorption band below the 400 nm in wavelength (UV region), which is consistent with reported the literature[52–54]. The hydrothermal synthesis done, allowed the formation of $CeO_2$ nanoparticles with an average diameter of 89 nm. SEM analysis (discussed deeply on section 4.1.4) confirmed the presence of $CeO_2$ nanoparticles within the nanofibrous structures. Sonication treatment performed on polymer-ceria nanoparticles mixtures allowed a well dispersion of ceria nanoparticles, hence no surfactant was used for dispersion. According to recent studies, ceria nanoparticles display a good UV blocking (200-350 nm), making this kind of nanoparticles a potential to be used as UV blocker wearable film[53]. In addition, in combination with excellent UV blocking characteristics of nanoscaled chitosan (nanoparticles and nanofibers)[55,56], complexes of this polymer doped with ceria nanoparticles can be applied as an attractive nanocomposite for several biomedical application including UV skin protectors and enhanced wound healing films.

### 4.1.2 Fourier transform infrared spectroscopy

FTIR spectra of doped ceria nanoparticles PVA nanofibers is shown on Figure 4.2. Characteristics peaks for this sample are located at 3267, 2934, 2906, 2852, 1644, 1412, 1323, 1084, 916 and 829 $cm^{-1}$ in wavenumber. The peak located at 3267 $cm^{-1}$ is associated with stretching vibrations of $OH^-$, this is

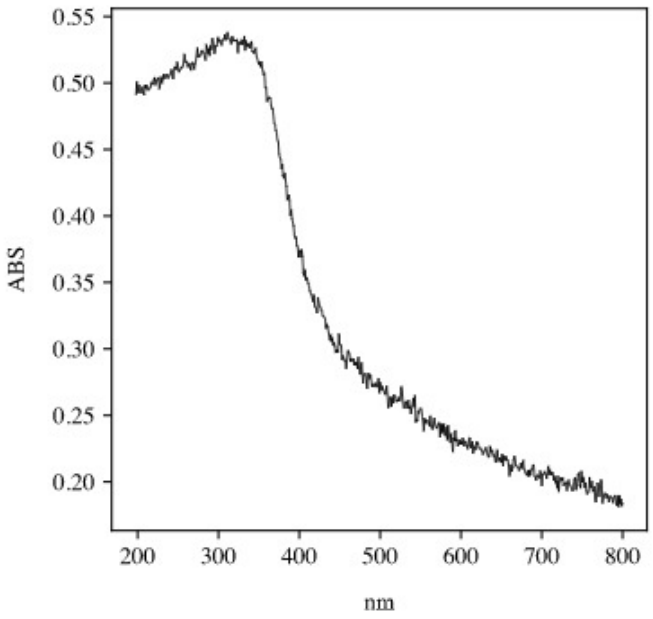


Figure 4.1: UV/vis spectra of synthesized cerium oxide nanoparticles. It shows a strong peak located at 312 nm.

due to the strong hydrogen bonds present on water molecules[57], as water was used as solvent for PVA polymer solution. Also, the band located at between 2852 and 2934 $cm^{-1}$ is attributed to the asymmetric stretching vibration of the alkali group (CH). Peaks located at 1644, 1323, 1084, 916 and 839 $cm^{-1}$, are associated with C=O carbonyl stretching vibration, the C-H bending vibrations of $CH_2$, C-H deformation, C-O stretching vibrations and C-C stretching vibration respectively[58,59]. The less intensity peak located below 500 $cm^{-1}$ is attributed to the replacements of hydrogens (H) with $CeO_2$[60]. In general, all displayed transmittance bands are associated with characteristic peaks for PVA nanofibers according to the reported bibliography.

In Figure 4.3 are shown the FTIR spectra of doped ceria nanoparticles PVA/chitosan (70/30) nanofibers. Characteristic peaks are located at 3283, 2938, 1662, 1424, 1328, 1092, 846 and 617 $cm^{-1}$. As for the previous explained graph, the peaks at 3283 $cm^{-1}$ is attributed to the hydroxil ($OH^-$) and amino (-NH) of chitosan stretching vibrations[61]. Peak located at 2938 $cm^{-1}$ refers to alkaly (CH) groups. Peak at 1662 $cm^{-1}$ concerns to the formation of amine groups (C=N) related to chitosan composition[62]. Also, peaks at 1424, 1328, 1092, 846 and 617 $cm^{-1}$ are strongly associated to carboxylic acid vibrations, C-H vibrations, C-H deformation due to crystallization of chitosan, C-C stretching vibration and interaction of $CeO_2$ within the nanofibrous structure[61,62]. In Figure 4.4 a comparison between doped ceria nanoparticles PVA and PVA/chitosan (70/30) nanofibers is shown. A clearly shifting to a higher wavenumber is evident because of the overlapping of amino and amine I group in the doped ceria nanoparticles PVA/chitosan nanofibers; additionally, a decrease in the intensity of transmittance is observable for doped PVA/chitosan nanofibers due to the phenomenon explained before[57].

### 4.1.3 Raman spectroscopy

Figure 4.5 shows the Raman spectra of bare PVA and PVA doped with different percentages of ceria nanoparticles. Two well defined strong peaks can be easily appreciated at wavenumbers of 2914 and 1442 $cm^{-1}$, these peaks are associated to stretching vibrations of -$CH_2$ and -CH groups, respectively. Figure 4.6, depicts the expanded regions of the Raman spectra of PVA and doped ceria nanoparticles PVA nanofibers, comprehending band from around $cm^{-1}$ to 1450 $cm^{-1}$[63]. In this enlarged region 3 more peaks at 1147, 926 and 862 $cm^{-1}$ can be ascribed for bare PVA nanofibers to -$CH_3$ stretching, C-C stretching vibrations and -$CH_2$ deformation vibrations, respectively[63].
Additionally, a low intensity peak located at 485 $cm^{-1}$ can be distinguished in samples containing the 3 different doping of ceria nanoparticles. What is more, the intensity of peaks increases as the doping of ceria nanoparticles increases, which is consistent with reported literature[64]. Variations of the $OH^-$ vibrational Raman signal can be seen as nanofibers were doped with ceria nanoparticles in fig 4.5, this

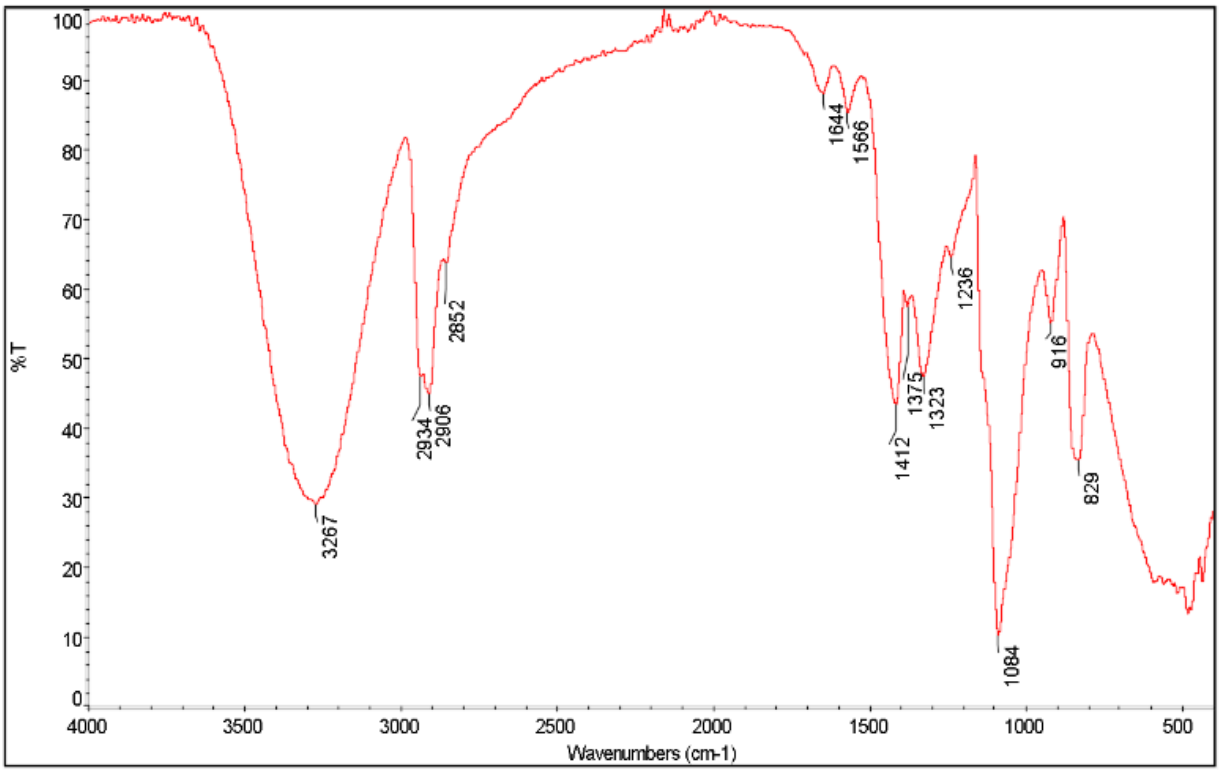


Figure 4.2: FTIR spectra of doped ceria nanoparticles PVA nanofibers

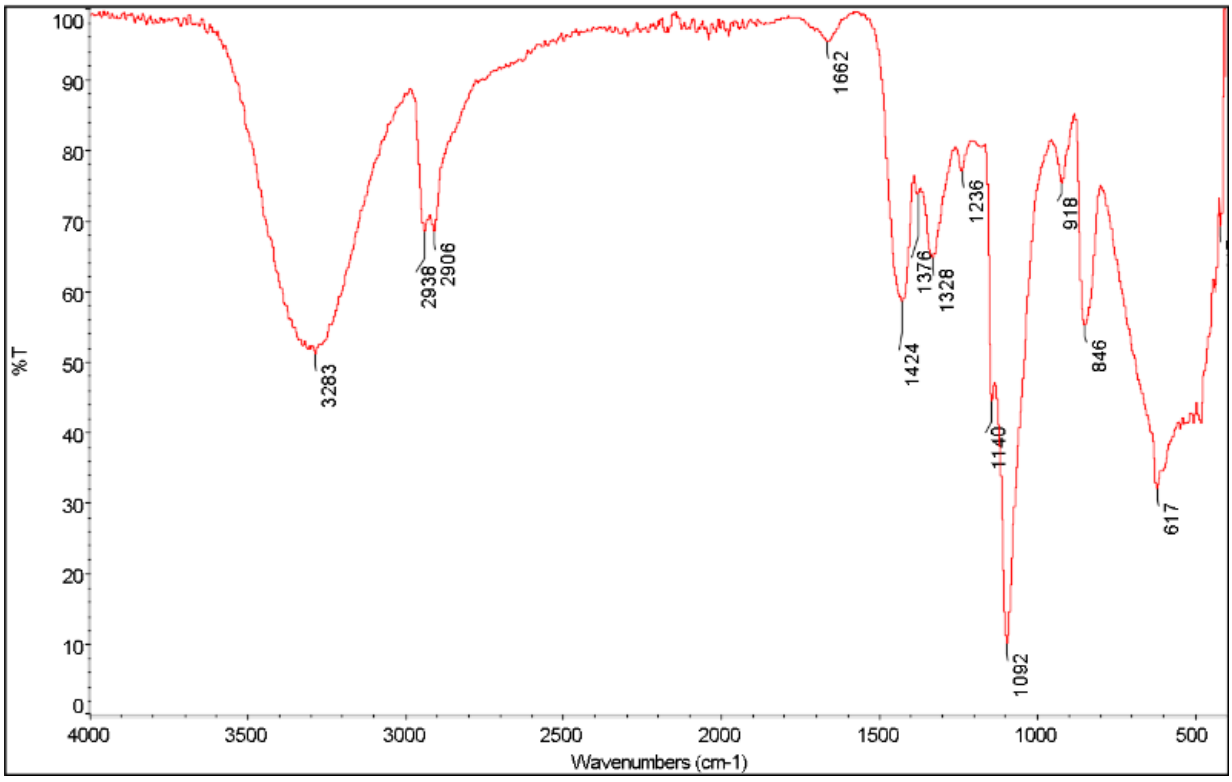


Figure 4.3: FTIR spectra of doped ceria nanoparticles PVA/chitosan (70/30) nanofibers

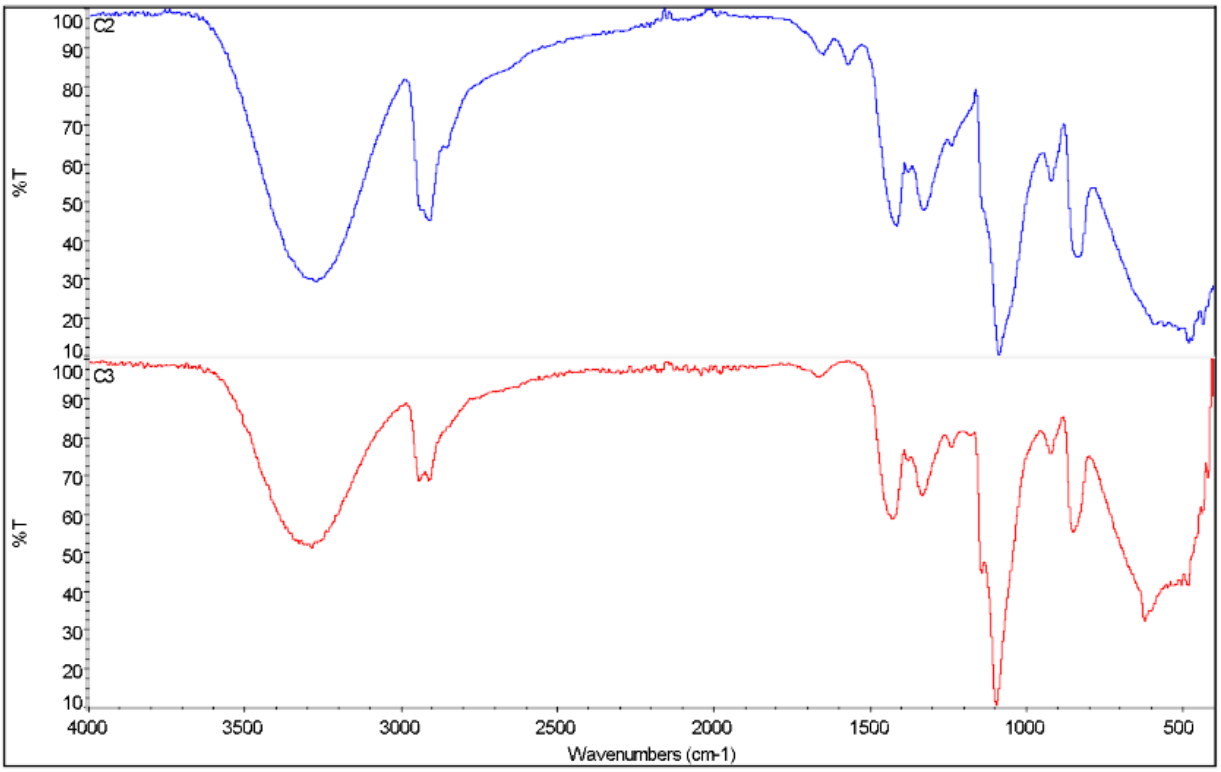


Figure 4.4: FTIR comparison spectra between doped PVA and doped PVA/chitosan (70/30) nanofibers

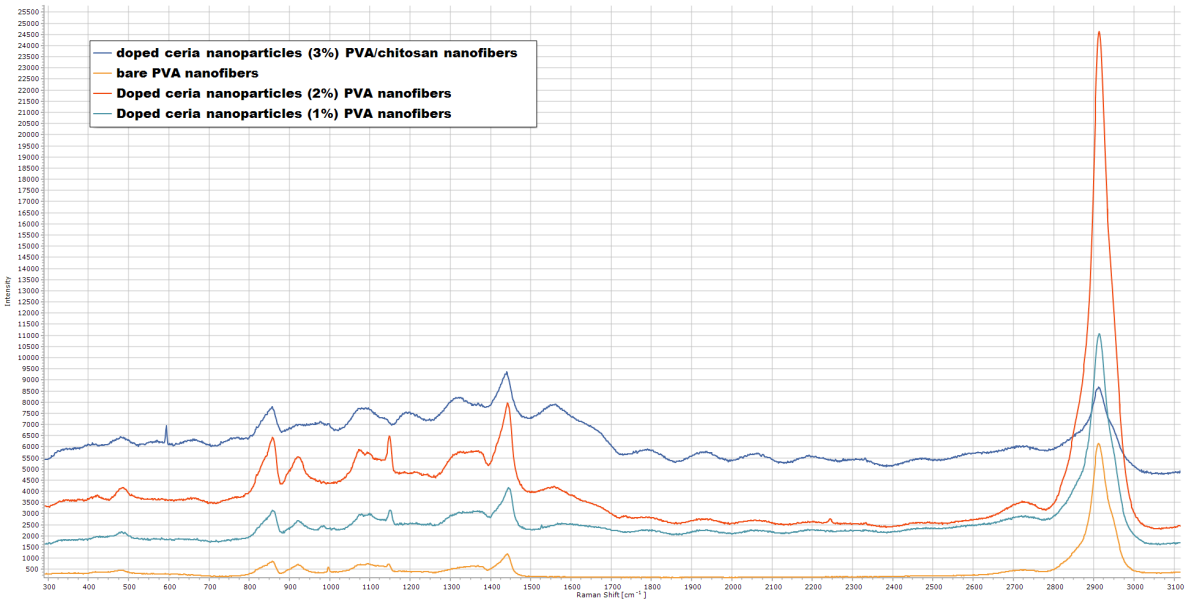


Figure 4.5: Raman spectra showing bare PVA and 1%, 2% and 3% doped ceria nanoparticles PVA nanofibers

is related to the replacing of $OH^-$ groups with ceria[64]. A sharp peak is located at 595 $cm^{-1}$ in 3% doped ceria nanoparticles PVA nanofibers, and associated with the D (defects) band contributions of ceria nanocrystallites[64–66]. The presence of this band in the highest doping percentages is attributed to the mayor presence of ceria nanoparticles in this sample.

In Figures 4.7 and 4.8 are displayed the Raman spectra of PVA/chitosan (70/30) and doped ceria nanoparticles (1%, 2% and 3%) PVA/chitosan (70/30) nanofibers. As in PVA and doped PVA nanofibers, 2 stronger-sharp peaks are present at 2917 and 1451 $cm^{-1}$, associated with -$CH_2$ and-CH stretching vibrations, characteristic peaks of both PVA and chitosan nanofibers. Also it can be seen an overlapping of -CNH bending region of chitosan with -$CH_3$ stretching vibration of PVA[67]. Another characteristic band for PVA and PVA/chitosan (70/30) nanofibers is located between 907 and 967 $cm^{-1}$, that indicates C-C stretching vibrations, as well as a peak at 864 $cm^{-1}$ that is ascribed to -$CH_2$ deformation vibrations[67]. Overlapping of amino and amide I and III groups present in chitosan are displayed as a series of trans-amide peaks between 960 and 1100 $cm^{-1}$ that make the spectra shift towards a higher wavenumber[67–69]. Doped ceria nanoparticles PVA/chitosan (70/30) nanofibers samples displayed a Raman peak located at 467 $cm^1$ that confirms the interaction of ceria nanoparticles within the polymeric structure.

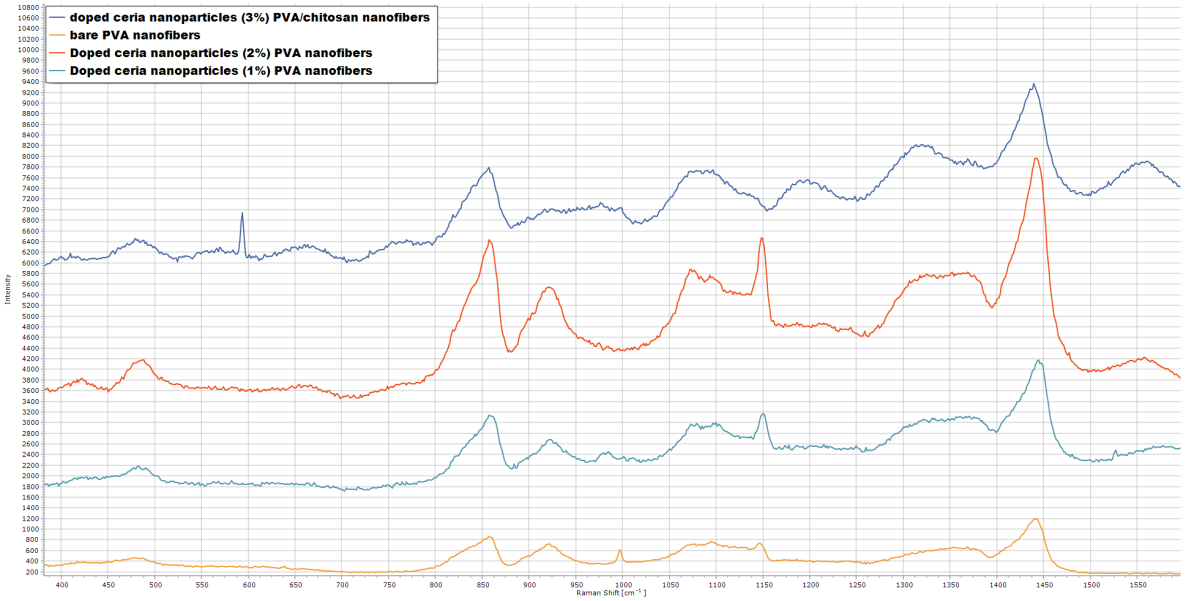


Figure 4.6: Expanded regions of Raman spectra of pure and doped PVA nanofibers

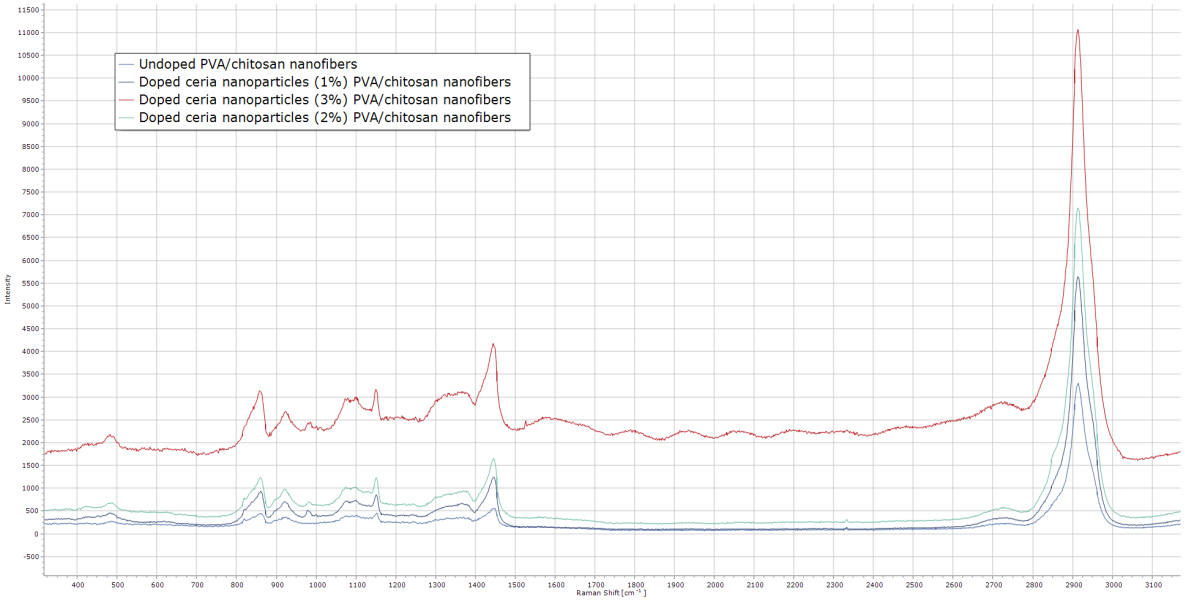


Figure 4.7: Raman spectra showing bare PVA/chitosan (70/30) and 1%, 2% and 3% doped ceria nanoparticles PVA/chitosan (70/30) nanofibers.

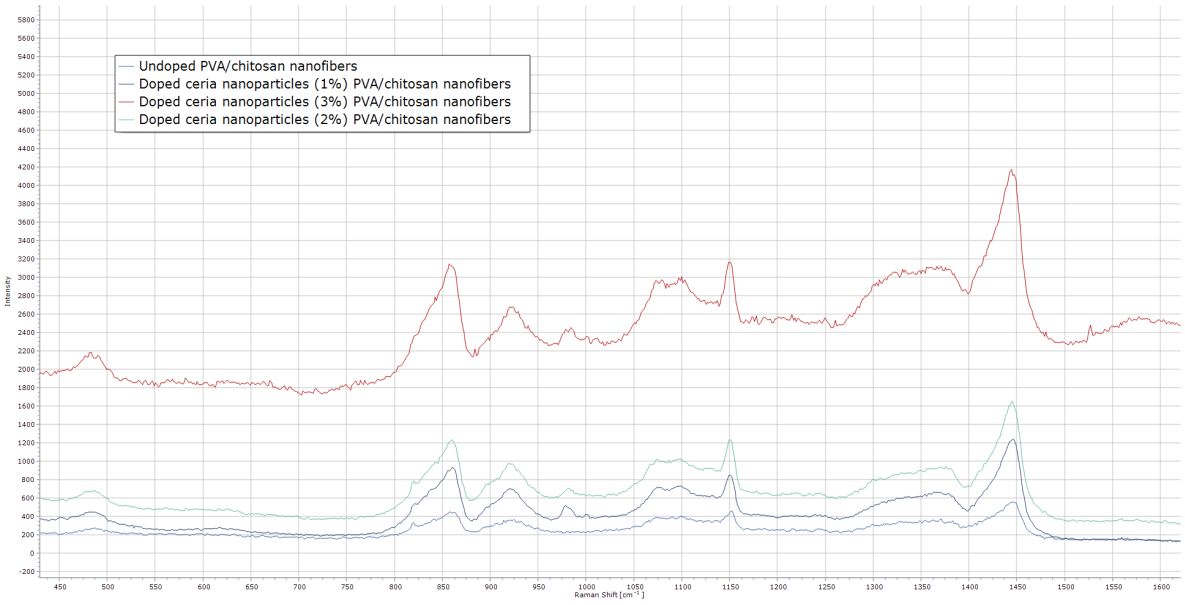


Figure 4.8: Expanded regions of Raman spectra of pure and doped PVA/chitosan (70/30) nanofibers.

### 4.1.4 Scanning electron microscopy (SEM) and Energy dispersive X-ray spectroscopy (EDX)

The resultant morphological structure as well as the chemical composition of bare PVA, and doped ceria ($CeO_2$) nanoparticles PVA and PVA/chitosan complexes were studied by SEM and EDX analysis. SEM micrographs of bare PVA and PVA nanofibers with different doping percentages of ceria nanoparticles and magnifications are presented in Figures 4.9 and 4.10, respectively. Pure PVA nanofibers are shown as semi-folded fibers with an average diameter of 367 nm. These nanofibers exhibited a smooth and beats-free surface. Alignment and surface characteristics of the nanofibers give information related to the spinning conditions. In this case, non-alignment implies that voltage used for electrospinning of nanofibers could be increased. Even the distance from the spinneret to the collector could have been increased as no structural damage (or broken fibers) is appreciated on the micrograph. On Figure 4.10 doped ceria nanoparticles can be distinguished as brighter points on the surface of nanofibers, as elements with higher atomic number displays with less contrast than lower atomic number elements.

On Figure 4.10a, 4.10b, 4.10c and 4.10d ceria nanoparticles are well dispersed on the nanofibrous mat, and have an average diameter of 56 nm. There exist and exception at certain spots of Figure 4.10b, where an agglomeration of ceria nanoparticles can be observed. This is mainly due to the exertion of a

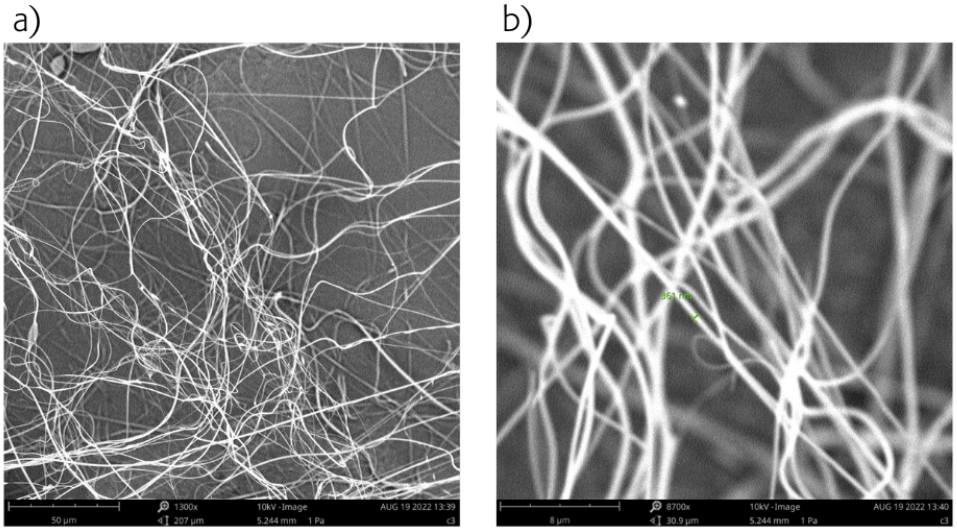


Figure 4.9: SEM micrographs of bare PVA nanofibers with a magnification of 1650x in a) and with a magnification of 8700x in b).

high electric filed during the electrospinning process, and susceptibility of ceria nanoparticles to interact with the electric field[70]. Average diameter of doped ceria nanoparticles PVA nanofibers was 179 nm. Also, better alignment of nanofibers can be clearly appreciated. In this case, ceria nanoparticles provided sufficient body stability to the nanofibrous matrix, making them maintain a certain alignment[70–72]. Some droplets can be seen on figure 4.10a and 4.10d, this was produced because repeatability of experiments was not reachable as weather conditions in the laboratory (temperature and humidity) varied significantly in time. Hence, a stable Taylor's cone could not be achieved.

SEM micrograph at different magnifications of PVA/chitosan (70/30) nanofibers (Figure 4.11) and doped ceria nanoparticles PVA/chitosan (70/30) nanofibers (Figures 4.11b-d) are shown on Figure 4.11. Smooth and beats-free nanofibers with an average diameter of 389 nm were fabricated. All the contrary to PVA/chitosan (70/30) nanofibers; doped ceria nanoparticles PVA/chitosan (70/30) nanofibers exhibited a better alignment again, mainly due to the stability that provide ceria nanoparticles within the structure. It could be appreciated that, as the ceria nanoparticles concentration was increased, the diameter of the nanofiber was reduced. This, again, implies that the interaction of the electric field with ceria nanoparticles allows the nanofibers to elongated due to the exerted electric forces[70].

Figure 4.12 shows an energy dispersive x-ray spectroscopy analysis of a)doped ceria nanoparticles PVA nanofibers and b) doped ceria nanoparticles PVA/chitosan (70/30) nanofibers. Percentages of ceria are shown as weight percentages. A majority proportion of carbon and oxygen atoms are displayed as they are the predominant elements in both PVA and PVA/chitosan (70/30) nanofibers. A trace of sulfur is shown on Figure 4.12a because the source of cerium atoms was cerium sulfate. However, the residual sulfur quantity was so minimal that FTIR and Raman spectroscopy experiments were not affected by it and all the peaks were congruent with reported bibliography.

### 4.1.5 Antibacterial and antifungal tests

The bacterial and fungal inhibition tests of the doped ceria nanoparticles PVA and PVA/chitosan (70/30) nanofibers against *E. coli ATCC 25922* and *Candida albicans* were performed by the disc diffusion susceptibility test after 24 h incubation. All nanofibers were cut to an approximately size of 4 mm × 4 mm for the antibacterial and antifungal experiments. To confirm whether doped ceria nanoparticles PVA/Chitosan (70/30) and PVA nanofibers have an effective antibacterial and antifungal activity, pure PVA nanofibers and acetic acid (solvent of chitosan) were used as negative controls. As shown in Fig. 4.13 and in Fig. 4.14, both *E. coli ATCC 25922* (Fig. 4.13) and *Candida albicans* (Fig. 4.14) clearly showed a zone of inhibited growth of the bacteria and fungi around the doped ceria nanoparticles PVA/Chitosan (70/30) and doped ceria nanoparticles PVA nanofibers. In contrast, in the absence of ceria nanoparticles and chitosan, pure PVA nanofibers and acetic acid negative controls showed nor antibacterial or antifungal activity, without zone of inhibition. It distinctly demonstrated that bacterial and fungal growth was inhibited depending upon the presence of ceria nanoparticles and chitosan in the fiber. These results suggest that *E. coli* and *Candida albicans* are affected by ceria nanoparticles and chitosan, as they are lethal to these particular bacteria and fungi. First of all, Muzzarelli et al. (2019)[73] tested the bactericidal effect of chitosan on 289 strains of Gram-positive and Gram-negative bacteria, observing morphological damage, weakening and thinning of cell walls, modifications and disappearance of internal cell structures. It has been reported that chitosan exerts an effective control on the growth of filamentous fungi and yeast[74]. Also, Hardiansyah et al. (2015)[75] demonstrated that chitosan blended poly(lactic acid) nanofibers content above 3.2 wt% killed *E. coli* on the first day. This could be explained due to the presence of highly positively charged chitosan, which is known to hinder the biosynthesis and energy transport through the cell wall and killed the bacteria[76]. The positively charged $-NH^{3+}$ would bind to the negatively charged cell walls of *E. coli* and cause their enzymes to break down[75]. This is in accordance with the previous research that confirmed chitosan exhibiting the ability to inhibit the growth of several Gram-positive and Gram-negative bacteria and has high antimicrobial activity against *E. coli*[76,77]. Furthermore, a report of chitosan-PVA nanofibers showed a high antimicrobial activity against E. coli for larger diameters, possibly due to a more

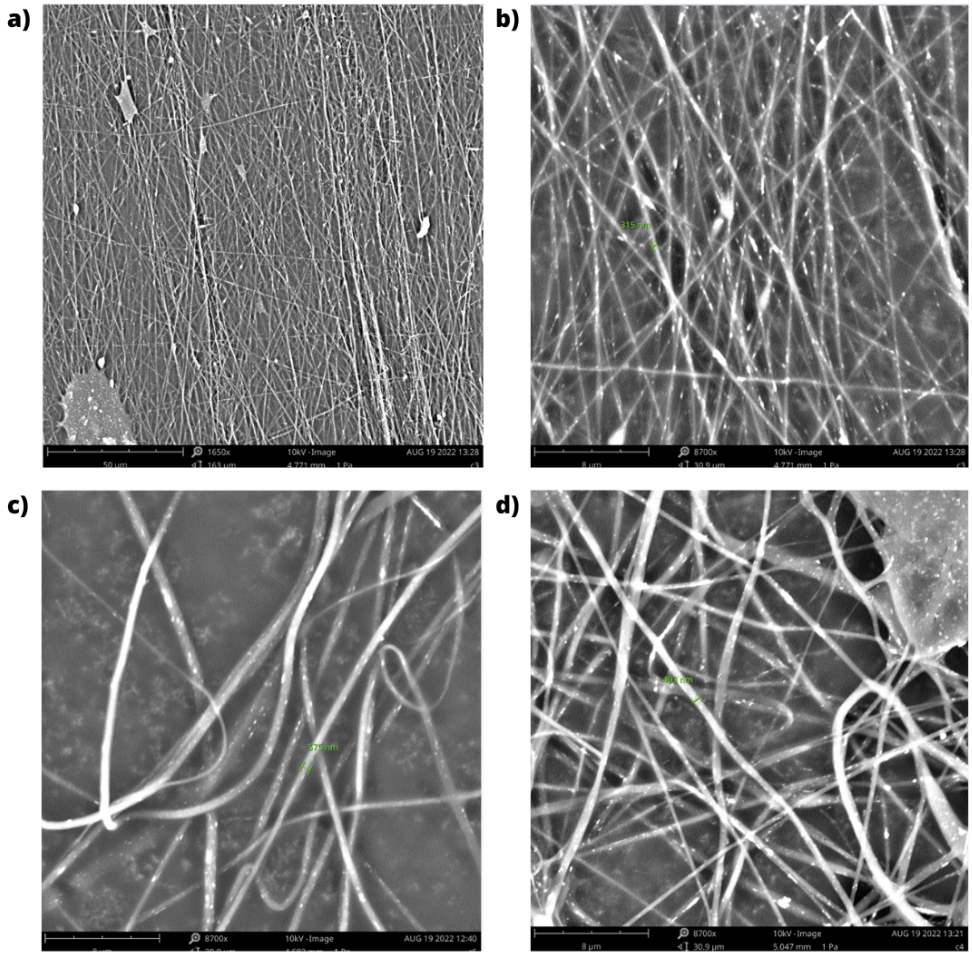


Figure 4.10: SEM micrographs of a) and b) 1 % doped ceria nanoparticles PVA nanofibers at different magnifications, c) 2% doped ceria nanoparticles PVA nanofibers with a magnification of 8700x, and d) 3% doped ceria nanoparticles PVA nanofibers with a magnification of 8700x. Doped ceria nanoparticles can be seen as brighter points within the nanofibrous structure in all micrographs

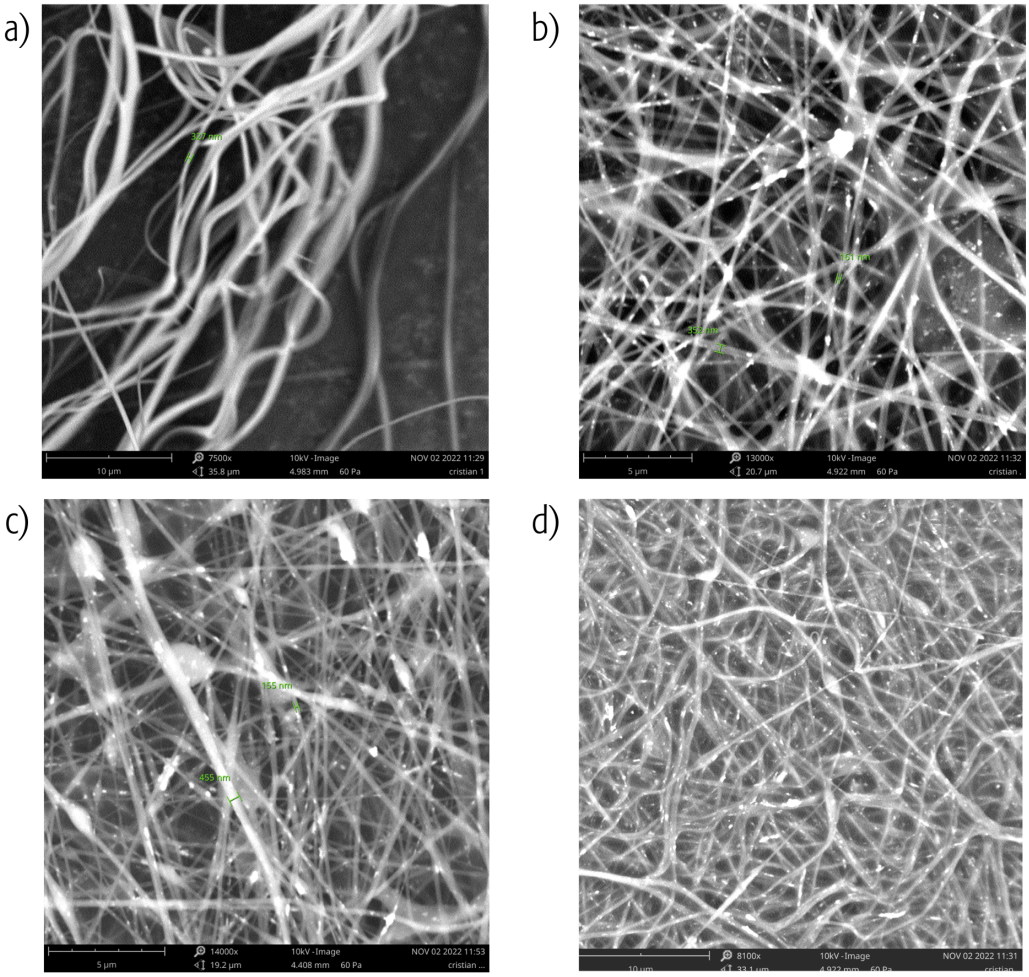


Figure 4.11: SEM micrographs showing (a) PVA/chitosan (70/30) and (b) 1%, (c) 2% and (d) 3% doped ceria nanoparticles PVA/chitosan (70/30) nanofibers.

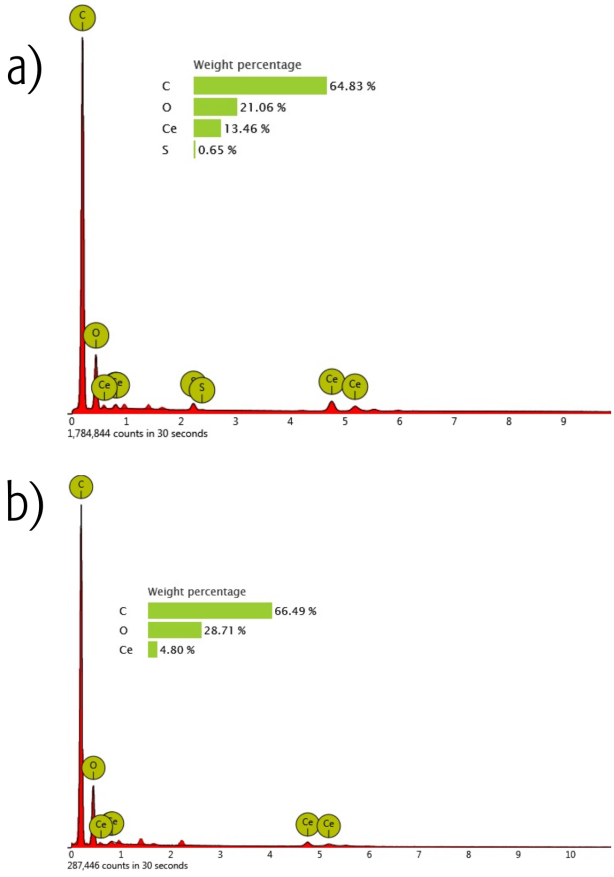


Figure 4.12: EDX analysis of doped ceria nanoparticles a)PVA and b)PVA/chitosan (70/30) nanofibers.

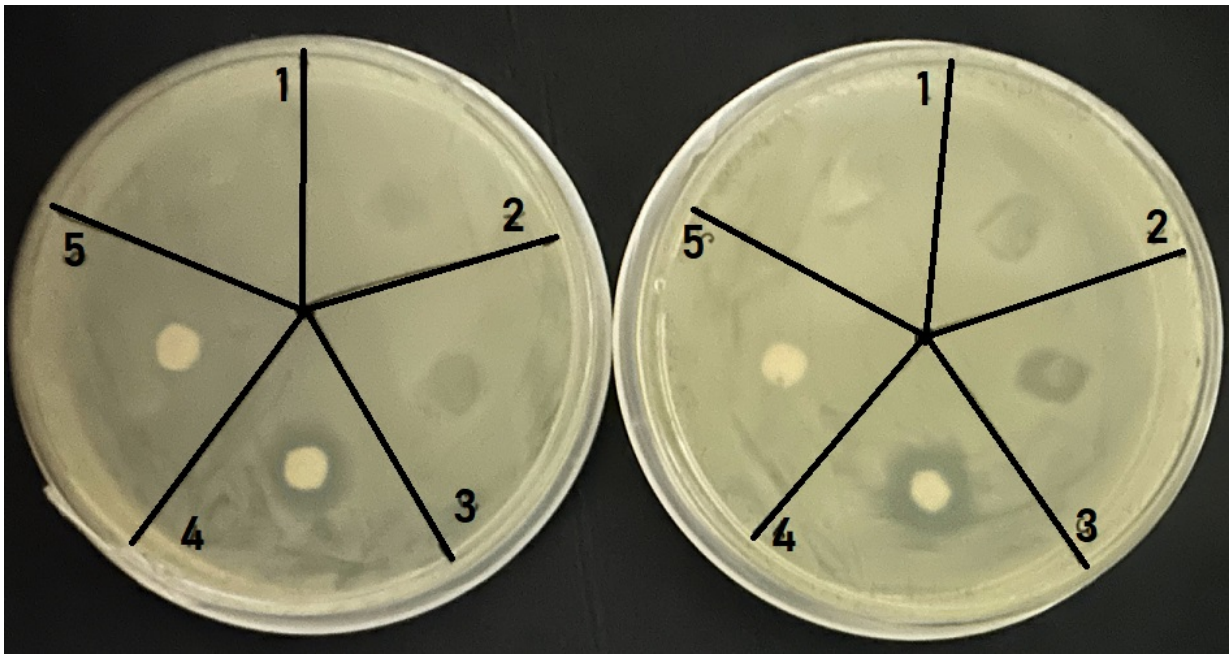


Figure 4.13: Antibacterial test of doped ceria nanoparticles PVA and PVA/chitosan (70/30) nanofibers against *E. coli ATCC 25922*. Labels 1= bare PVA nanofibers negative control; 2= doped ceria nanoparticles PVA nanofibers treatment; 3= doped ceria nanoparticles PVA/chitosan (70/30) nanofibers treatment; 4= (1:1000) dilution of Nourseothricin (240 $\mu$g/mL) positive control; and 5= 3% wt solution of acetic acid.

effective contact surface area and a greater presence of amino groups to carry out the inhibition of microbial growth. The antibacterial activity of chitosan nanofibers may also be due to the release of small chitosan oligomers that could penetrate bacterial cells and interact with DNA[74]. Additionally, the incorporation of ceria nanoparticles in electrospun chitosan nanofibers could suggest an improvement in the antibacterial performance. The ceria nanoparticles, due to their outstanding physical and chemical properties, have been promising for biomedical applications for their demonstrated antibacterial and antifungal activities[78,79]. For studies of antifungal activity[79], ceria nanoparticles were used against clinical strains of *Candida albicans*, where the minimum inhibitory concentration of ceria nanoparticles (0.12 – 0.48 $\mu$g/mL) was lower than fluconazole drug (1.75 – 25 $\mu$g/mL) against clinical strains of C. albicans. This work conclude that ceria nanoparticles have potential and effective antifungal activity against isolates of *C. albicans* compared to fluconazole. Also, there are reported studies that confirm major growth inhibition and antibacterial activity of ceria nanoparticles against the gram-negative bacterium *Staphylococcus aeruginosa* and gram-positive bacterium *Staphylococcus aureus*[79,80].

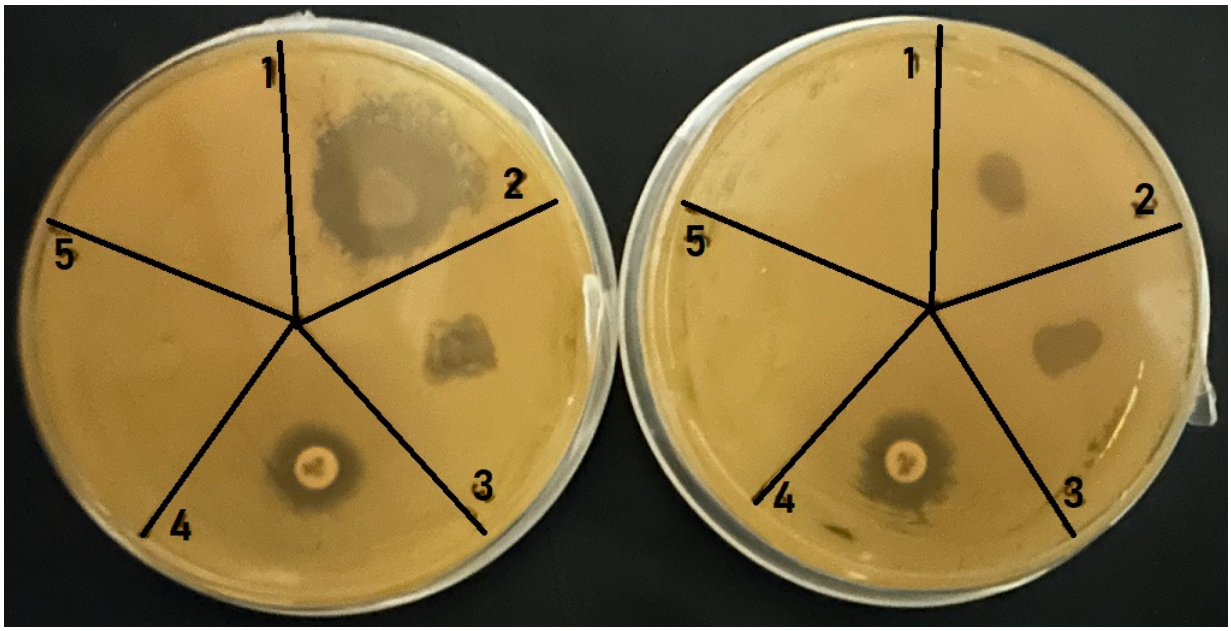


Figure 4.14: Antifungal test of doped ceria nanoparticles PVA and PVA/chitosan (70/30) nanofibers against *Candida albicans*. Labels 1= bare PVA nanofibers negative control; 2= doped ceria nanoparticles PVA nanofibers treatment; 3= doped ceria nanoparticles PVA/chitosan (70/30) nanofibers treatment; 4= (1:1000) dilution of Fluconazole (25 $\mu$g/mL) positive control; and 5= 3% wt solution of acetic acid.

# Chapter 5

# Conclusions & Outlook

The present work reported the synthesis of ceria nanoparticles, PVA and chitosan polymeric solutions, and the fabrication of PVA, PVA/chitosan (70/30), doped ceria nanoparticles PVA and doped ceria nanoparticles PVA/chitosan (70/30) electrospun nanofibers. The electrospinning technique is a relative low cost method that, with specific modifications, can be used for scaled up mass production. The method use a high electric field to inject a polymer solution into a collector plate, achieving polymerization and formation of fibers in the micron or nano scale in the process. PVA was dissolved in water to form a 8% solution and chitosan was dissolved in 10% acetic acid to form a 4% solution. Ceria ($CeO_2$) nanoparticles were hydrothermally synthesized and then characterized by UV-vis spectroscopy and scanning electron microscopy. UV/vis analysis confirmed the presence of ceria nanoparticles, with a strong- prominent peak at 312 nm, which is consistent with reported studies. PVA/chitosan blend polymeric solutions at volume ratios of 0/100, 30/70, 50/50 and 70/30 were made. Doping of 1%, 2% and 3% of ceria nanoparticles were performed on both PVA and PVA/chitosan polymeric solutions. Electrospinning technique was applied to fabricate PVA, PVA/chitosan (70/30), and doped ceria nanoparticles PVA and PVA/chitosan (70/30) nanofibers. The volume ratio of PVA/chitosan used for the effective fabrication of nanofibers was (70/30), other volume ratios did not result in the development of nanofibers. Reported studies have found out difficult the fabrication of bare acetic acid soluble chitosan nanofibers, and recommend to blend chitosan polymeric solution with other more "electrospinneable" polymers, such as PVA, PLGA or pluronic F-127. A total of 42 electrospinning trials were done in order to find out the optimal polymers and machine parameters to produce nanofibers. Fabricated nanofibers were characterized by FTIR and Raman spectroscopy. Resultant FTIR analysis for doped PVA and PVA/chitosan (70/30) nanofibers displayed prominent peaks at 3267 and 1089 $cm^{-1}$, which are congruent with bibliography and corresponds to hydroxyl groups stretching vibrations and C-H vibrations, respectively . In the same way, Raman analysis resulted in strong and

sharp characteristic peaks at 2912 and 1442 $cm^{-1}$, which are consistent with literature for both PVA and PVA/chitosan nanofibers. The wave numbers previously mentioned, correspond to -$CH_2$ and -CH stretching vibrations, respectively. Also, for doped ceria nanoparticles PVA/chitosan blend nanofibers, it could be observed a overlapping of the amino I and II groups, due to the predominant presence of PVA within the blend polymeric solution. SEM and EDX analysis gave good results in terms of the morphology and composition of the nanofibrous mats. Average diameters for PVA, PVA/chitosan (70/30), doped PVA and doped PVA/chitosan (70/30) nanofibers were 367, 389, 179 and 182 nm, respectively. It can be also concluded that, for ceria nanoparticles doped systems, the average diameter of the nanofiber decreased in comparison with undoped nanofibers. EDX analysis confirmed the presence of ceria nanoparticles within the nanofibers. Antibacterial and antifungal susceptibility assays of doped and undoped nanofibers on *E. coli ATCC 25922* and *Candida albicans* were developed and the results demonstrated that doped ceria nanoparticles PVA nanofibers and doped ceria nanoparticles PVA/chitosan (70/30) nanofibers inhibited both bacterial and fungal growth. Results of the biological assays were confirmed by using highly specific drugs (Fluconazole for fungal growth and Nourseothricin for bacterial growth) as positive controls, diluted acetic acid and bare PVA nanofibers were used as negative controls in both assays. Acetic acid, which is the solvent for chitosan polymeric solution, was used to assure that fungal and bacterial inhibition produced by doped ceria nanoparticles PVA/chitosan (70/30) nanofibers were inherent of chitosan and ceria nanoparticles. Bare PVA nanofibers negative controls were used to prove that inhibition presented in doped ceria nanoparticles PVA nanofibers is due to the ceria nanoparticles. Several studies have to be performed in order to study the nanofibers synthesized in depth. For instance, differential scanning calorimetry (DSC) and thermogravimetric analysis (TGA) must be done to study glass transition temperature of the nanofibers. This would allow us to know an approximation of the actual fraction of PVA/chitosan present in the nanofibers. Also, quenching, swelling, drug delivery, biocompatibility, antiinflamatory and cytotoxicity tests must be performed in order to study the capability of the synthesized nanofibers to be used as a biomaterial.

# Bibliography


[1] Zhong, S.; Zhang, Y.; Lim, C. Tissue scaffolds for skin wound healing and dermal reconstruction. *Wiley Interdisciplinary Reviews: Nanomedicine and Nanobiotechnology* **2010**, *2*, 510–525.

[2] Hutmacher, D. W. Scaffolds in tissue engineering bone and cartilage. *Biomaterials* **2000**, *21*, 2529–2543.

[3] Hench, L.; Jones, J. *Biomaterials, artificial organs and tissue engineering*; Elsevier, 2005.

[4] Shoichet, M. S. Polymer scaffolds for biomaterials applications. *Macromolecules* **2010**, *43*, 581–591.

[5] Hosseini, M.; Shafiee, A. Engineering bioactive scaffolds for skin regeneration. *Small* **2021**, *17*, 2101384.

[6] Ben Khadra, Y.; Ferrario, C.; Di Benedetto, C.; Said, K.; Bonasoro, F.; Candia Carnevali, M. D.; Sugni, M. Wound repair during arm regeneration in the red starfish E chinaster sepositus. *Wound Repair and Regeneration* **2015**, *23*, 611–622.

[7] Da, L.-C.; Huang, Y.-Z.; Xie, H.-Q.; Zheng, B.-H.; Huang, Y.-C.; Du, S.-R. Membranous Extracellular Matrix-Based Scaffolds for Skin Wound Healing. *Pharmaceutics* **2021**, *13*, 1796.

[8] Kundu, B.; Rajkhowa, R.; Kundu, S. C.; Wang, X. Silk fibroin biomaterials for tissue regenerations. *Advanced drug delivery reviews* **2013**, *65*, 457–470.

[9] Sultana, N. *Biodegradable polymer-based scaffolds for bone tissue engineering*; Springer Berlin, Germany:, 2013.

[10] Ninan, N.; Muthiah, M.; Park, I.-K.; Wong, T. W.; Thomas, S.; Grohens, Y. Natural polymer/inorganic material based hybrid scaffolds for skin wound healing. *Polymer Reviews* **2015**, *55*, 453–490.

[11] Salim, S. A.; Taha, A. A.; Khozemy, E. E.; EL-Moslamy, S. H.; Kamoun, E. A. Electrospun zinc-based metal organic framework loaded-PVA/chitosan/hyaluronic acid interfaces in antimicrobial composite nanofibers scaffold for bone regeneration applications. *Journal of Drug Delivery Science and Technology* **2022**, *76*, 103823.

[12] Bhardwaj, N.; Kundu, S. C. Electrospinning: a fascinating fiber fabrication technique. *Biotechnology advances* **2010**, *28*, 325–347.

[13] Rahdar, A.; Aliahmad, M.; Samani, M.; HeidariMajd, M.; Susan, M. A. B. H. Synthesis and characterization of highly efficacious Fe-doped ceria nanoparticles for cytotoxic and antifungal activity. *Ceramics International* **2019**, *45*, 7950–7955.

[14] Panda, S. R.; Singh, R. K.; Priyadarshini, B.; Rath, P. P.; Parhi, P. K.; Sahoo, T.; Mandal, D.; Sahoo, T. R. Nanoceria: A rare-earth nanoparticle as a promising anti-cancer therapeutic agent in colon cancer. *Materials Science in Semiconductor Processing* **2019**, *104*, 104669.

[15] Marghoob, M. U.; Noureen, A.; Raza, A.; Khan, W. S.; Iftikhar, M.; Sher, F. Synthesis and toxicity assessment of environment friendly high yield ceria nanoparticles for biosafety. *Journal of Environmental Chemical Engineering* **2022**, *10*, 107029.

[16] others,, *et al.* The advances of ceria nanoparticles for biomedical applications in orthopaedics. *International journal of nanomedicine* **2020**, *15*, 7199.

[17] Torres-Romero, A.; Cajero-Juarez, M.; Nunez-Anita, R.; Contreras-Garcia, M. Ceria-doped titania nanoparticles as drug delivery system. *Journal of Nanoscience and Nanotechnology* **2020**, *20*, 3971–3980.

[18] Woo, S.; Lee, J.; Lee, D. S.; Kim, J. K.; Lim, B. Electrospun carbon nanofibers with embedded co-ceria nanoparticles for efficient hydrogen evolution and overall water splitting. *Materials* **2020**, *13*, 856.

[19] Motasadizadeh, H.; Azizi, S.; Shaabani, A.; Sarvestani, M. G.; Sedghi, R.; Dinarvand, R. Development of PVA/Chitosan-g-Poly (N-vinyl imidazole)/TiO2/curcumin nanofibers as high-performance wound dressing. *Carbohydrate Polymers* **2022**, *296*, 119956.

[20] Kas, H. S. Chitosan: properties, preparations and application to microparticulate systems. *Journal of microencapsulation* **1997**, *14*, 689–711.

[21] Ramsden, J. *Nanotechnology: an introduction*; William Andrew, 2016.

[22] Mohanraj, V.; Chen, Y. Nanoparticles-a review. *Tropical journal of pharmaceutical research* **2006**, *5*, 561–573.

[23] Langer, R. Biomaterials in drug delivery and tissue engineering: one laboratory's experience. *Accounts of Chemical Research* **2000**, *33*, 94–101.

[24] Singh, R.; Nalwa, H. S. Medical applications of nanoparticles in biological imaging, cell labeling, antimicrobial agents, and anticancer nanodrugs. *Journal of biomedical nanotechnology* **2011**, *7*, 489–503.

[25] Yadid, M.; Feiner, R.; Dvir, T. Gold nanoparticle-integrated scaffolds for tissue engineering and regenerative medicine. *Nano letters* **2019**, *19*, 2198–2206.

[26] Senanayake, S. D.; Stacchiola, D.; Rodriguez, J. A. Unique properties of ceria nanoparticles supported on metals: novel inverse ceria/copper catalysts for CO oxidation and the water- gas shift reaction. *Accounts of Chemical Research* **2013**, *46*, 1702–1711.

[27] others,, *et al.* The advances of ceria nanoparticles for biomedical applications in orthopaedics. *International journal of nanomedicine* **2020**, *15*, 7199.

[28] Qi, L.; Xu, Z.; Jiang, X.; Hu, C.; Zou, X. Preparation and antibacterial activity of chitosan nanoparticles. *Carbohydrate research* **2004**, *339*, 2693–2700.

[29] Aranaz, I.; Alcántara, A. R.; Civera, M. C.; Arias, C.; Elorza, B.; Heras Caballero, A.; Acosta, N. Chitosan: An overview of its properties and applications. *Polymers* **2021**, *13*, 3256.

[30] prasanth Koppolu, B.; Zaharoff, D. A.; Smith, S. G.; Ravindranathan, S. Effect of Chitosan Properties on Immunoreactivity. *Marine Drugs* **2016**,

[31] Rinaudo, M. Chitin and chitosan: Properties and applications. *Progress in polymer science* **2006**, *31*, 603–632.

[32] Lee, D.-W.; Shirley, S. A.; Lockey, R. F.; Mohapatra, S. S. Thiolated chitosan nanoparticles enhance anti-inflammatory effects of intranasally delivered theophylline. *Respiratory research* **2006**, *7*, 1–10.

[33] Younes, I.; Rinaudo, M. Chitin and chitosan preparation from marine sources. Structure, properties and applications. *Marine drugs* **2015**, *13*, 1133–1174.

[34] Baker, M. I.; Walsh, S. P.; Schwartz, Z.; Boyan, B. D. A review of polyvinyl alcohol and its uses in cartilage and orthopedic applications. *Journal of Biomedical Materials Research Part B: Applied Biomaterials* **2012**, *100*, 1451–1457.

[35] Zeleny, J. The electrical discharge from liquid points, and a hydrostatic method of measuring the electric intensity at their surfaces. *Physical Review* **1914**, *3*, 69.

[36] Formhals, A.; Schreiber-Gastell, R. Apparatus for producing artificial filaments from material such as cellulose acetate. *Schreiber-Gastell, Richard* **1934**,

[37] Zussman, E.; Theron, A.; Yarin, A. Formation of nanofiber crossbars in electrospinning. *Applied Physics Letters* **2003**, *82*, 973–975.

[38] Luu, Y.; Kim, K.; Hsiao, B.; Chu, B.; Hadjiargyrou, M. Development of a nanostructured DNA delivery scaffold via electrospinning of PLGA and PLA–PEG block copolymers. *Journal of controlled release* **2003**, *89*, 341–353.

[39] Chew, S.; Wen, Y.; Dzenis, Y.; Leong, K. W. The role of electrospinning in the emerging field of nanomedicine. *Current pharmaceutical design* **2006**, *12*, 4751–4770.

[40] Leidy, R.; Ximena, Q.-C. M. Use of electrospinning technique to produce nanofibres for food industries: A perspective from regulations to characterisations. *Trends in Food Science & Technology* **2019**, *85*, 92–106.

[41] Liang, D.; Hsiao, B. S.; Chu, B. Functional electrospun nanofibrous scaffolds for biomedical applications. *Advanced drug delivery reviews* **2007**, *59*, 1392–1412.

[42] Zhou, W.; Apkarian, R.; Wang, Z. L.; Joy, D. *Scanning microscopy for nanotechnology*; Springer, 2006; pp 1–40.

[43] Abd Mutalib, M.; Rahman, M.; Othman, M.; Ismail, A.; Jaafar, J. *Membrane characterization*; Elsevier, 2017; pp 161–179.

[44] Kannan, M. Scanning electron microscopy: Principle, components and applications. *A textbook on fundamentals and applications of nanotechnology* **2018**, 81–92.

[45] Bracewell, R. N.; Bracewell, R. N. *The Fourier transform and its applications*; McGraw-Hill New York, 1986; Vol. 31999.

[46] Brigham, E. O.; Morrow, R. The fast Fourier transform. *IEEE spectrum* **1967**, *4*, 63–70.

[47] Berthomieu, C.; Hienerwadel, R. Fourier transform infrared (FTIR) spectroscopy. *Photosynthesis research* **2009**, *101*, 157–170.

[48] Movasaghi, Z.; Rehman, S.; ur Rehman, D. I. Fourier transform infrared (FTIR) spectroscopy of biological tissues. *Applied Spectroscopy Reviews* **2008**, *43*, 134–179.

[49] Ragavendran, P.; Sophia, D.; Arul Raj, C.; Gopalakrishnan, V. Functional group analysis of various extracts of Aerva lanata (L.,) by FTIR spectrum. *Pharmacologyonline* **2011**, *1*, 358–364.

[50] Liu, J.; Xiao, J.; Li, F.; Shi, Y.; Li, D.; Huang, Q. Chitosan-sodium alginate nanoparticle as a delivery system for $\varepsilon$-polylysine: Preparation, characterization and antimicrobial activity. *Food Control* **2018**, *91*, 302–310.

[51] Kim, K.-J.; Sung, W. S.; Suh, B. K.; Moon, S.-K.; Choi, J.-S.; Kim, J. G.; Lee, D. G. Antifungal activity and mode of action of silver nano-particles on Candida albicans. *Biometals* **2009**, *22*, 235–242.

[52] Dao, N. N.; Dai Luu, M.; Nguyen, Q. K.; Kim, B. S. UV absorption by cerium oxide nanoparticles/epoxy composite thin films. *Advances in Natural Sciences: Nanoscience and Nanotechnology* **2011**, *2*, 045013.

[53] Goharshadi, E. K.; Samiee, S.; Nancarrow, P. Fabrication of cerium oxide nanoparticles: Characterization and optical properties. *Journal of colloid and interface science* **2011**, *356*, 473–480.

[54] Hamidian, K.; Saberian, M. R.; Miri, A.; Sharifi, F.; Sarani, M. Doped and un-doped cerium oxide nanoparticles: Biosynthesis, characterization, and cytotoxic study. *Ceramics International* **2021**, *47*, 13895–13902.

[55] Roy, S.; Rhim, J.-W. Fabrication of chitosan-based functional nanocomposite films: Effect of quercetin-loaded chitosan nanoparticles. *Food Hydrocolloids* **2021**, *121*, 107065.

[56] Xia, Y.; Meng, F.; Wang, S.; Li, P.; Geng, C.; Zhang, X.; Zhou, Z.; Kong, F. Tough, antibacterial fish scale gelatin/chitosan film with excellent water vapor and UV-blocking performance comprising liquefied chitin and silica sol. *International Journal of Biological Macromolecules* **2022**,

[57] Ali, M.; Gherissi, A. Synthesis and characterization of the composite material PVA/chitosan/5% sorbitol with different ratio of chitosan. *Int. J. Mech. Mechatron. Eng* **2017**, *17*, 15–28.

[58] Salman, S. A.; Bakr, N. A.; Abduallah, S. S. Study of thermal decomposition and FTIR for PVA-AlCl composite films. *J. Eng. Appl. Sci* **2019**, *14*, 717–724.

[59] Qashou, S. I.; El-Zaidia, E.; Darwish, A.; Hanafy, T. Methylsilicon phthalocyanine hydroxide doped PVA films for optoelectronic applications: FTIR spectroscopy, electrical conductivity, linear and nonlinear optical studies. *Physica B: Condensed Matter* **2019**, *571*, 93–100.

[60] Petrescu, M.; Mitran, R.-A.; Matei, C.; Berger, D. Mesoporous silica-ceria composites as carriers for drug delivery systems. *Rev. Roum. Chim* **2016**, *61*, 557–563.

[61] Olewnik-Kruszkowska, E.; Gierszewska, M.; Jakubowska, E.; Tarach, I.; Sedlarik, V.; Pummerova, M. Antibacterial films based on PVA and PVA–chitosan modified with poly (hexamethylene guanidine). *Polymers* **2019**, *11*, 2093.

[62] Yu, Z.; Li, B.; Chu, J.; Zhang, P. Silica in situ enhanced PVA/chitosan biodegradable films for food packages. *Carbohydrate polymers* **2018**, *184*, 214–220.

[63] Shi, Y.; Xiong, D.; Li, J.; Wang, K.; Wang, N. In situ repair of graphene defects and enhancement of its reinforcement effect in polyvinyl alcohol hydrogels. *Rsc Advances* **2017**, *7*, 1045–1055.

[64] Loridant, S. Raman spectroscopy as a powerful tool to characterize ceria-based catalysts. *Catalysis Today* **2021**, *373*, 98–111.

[65] Taniguchi, T.; Watanabe, T.; Sugiyama, N.; Subramani, A.; Wagata, H.; Matsushita, N.; Yoshimura, M. Identifying defects in ceria-based nanocrystals by UV resonance Raman spectroscopy. *The Journal of Physical Chemistry C* **2009**, *113*, 19789–19793.

[66] Sartoretti, E.; Novara, C.; Giorgis, F.; Piumetti, M.; Bensaid, S.; Russo, N.; Fino, D. In situ Raman analyses of the soot oxidation reaction over nanostructured ceria-based catalysts. *Scientific reports* **2019**, *9*, 1–14.

[67] Nirmala, R.; Il, B. W.; Navamathavan, R.; El-Newehy, M. H.; Kim, H. Y. Preparation and characterizations of anisotropic chitosan nanofibers via electrospinning. *Macromolecular research* **2011**, *19*, 345–350.

[68] Filiz, B. C.; Elalmis, Y. B.; Bektaş, İ. S.; Figen, A. K. Fabrication of stable electrospun blended chitosan-poly (vinyl alcohol) nanofibers for designing naked-eye colorimetric glucose biosensor based on GOx/HRP. *International Journal of Biological Macromolecules* **2021**, *192*, 999–1012.

[69] Abbas, W. A.; Sharafeldin, I. M.; Omar, M. M.; Allam, N. K. Novel mineralized electrospun chitosan/PVA/TiO 2 nanofibrous composites for potential biomedical applications: Computational and experimental insights. *Nanoscale Advances* **2020**, *2*, 1512–1522.

[70] Takamura, H.; Kobayashi, J.; Takahashi, N.; Okada, M. Electrical conductivity of ceria nanoparticles under high pressure. *Journal of electroceramics* **2009**, *22*, 24–32.

[71] Wu, L.; Dey, S.; Gong, M.; Liu, F.; Castro, R. H. Surface segregation on manganese doped ceria nanoparticles and relationship with nanostability. *The Journal of Physical Chemistry C* **2014**, *118*, 30187–30196.

[72] Kalantari, K.; Mostafavi, E.; Saleh, B.; Soltantabar, P.; Webster, T. J. Chitosan/PVA hydrogels incorporated with green synthesized cerium oxide nanoparticles for wound healing applications. *European Polymer Journal* **2020**, *134*, 109853.

[73] Muzzarelli, R.; Tarsi, R.; Filippini, O.; Giovanetti, E.; Biagini, G.; Varaldo, P. Antimicrobial properties of N-carboxybutyl chitosan. *Antimicrobial agents and chemotherapy* **1990**, *34*, 2019–2023.

[74] Martínez-Camacho, A. P.; Cortez-Rocha, M. O.; Castillo-Ortega, M. M.; Burgos-Hernández, A.; Ezquerra-Brauer, J. M.; Plascencia-Jatomea, M. Antimicrobial activity of chitosan nanofibers obtained by electrospinning. *Polymer International* **2011**, *60*, 1663–1669.

[75] Hardiansyah, A.; Tanadi, H.; Yang, M.-C.; Liu, T.-Y. Electrospinning and antibacterial activity of chitosan-blended poly (lactic acid) nanofibers. *Journal of Polymer Research* **2015**, *22*, 1–10.

[76] Hu, S.-G.; Jou, C.-H.; Yang, M.-C. Surface grafting of polyester fiber with chitosan and the antibacterial activity of pathogenic bacteria. *Journal of Applied Polymer Science* **2002**, *86*, 2977–2983.

[77] Liu, N.; Chen, X.-G.; Park, H.-J.; Liu, C.-G.; Liu, C.-S.; Meng, X.-H.; Yu, L.-J. Effect of MW and concentration of chitosan on antibacterial activity of Escherichia coli. *Carbohydrate polymers* **2006**, *64*, 60–65.

[78] Rajeshkumar, S.; Naik, P. Synthesis and biomedical applications of cerium oxide nanoparticles–a review. *Biotechnology Reports* **2018**, *17*, 1–5.

[79] Zhang, Y.; Fu, T.; Yu, L.; Shen, F.; Wang, J.; Cui, K. Improving oxidation resistance of TZM alloy by deposited Si–MoSi2 composite coating with high silicon concentration. *Ceramics International* **2022**, *48*, 20895–20904.

[80] Magdalane, C. M.; Kaviyarasu, K.; Vijaya, J. J.; Siddhardha, B.; Jeyaraj, B. Photocatalytic activity of binary metal oxide nanocomposites of CeO2/CdO nanospheres: investigation of optical and antimicrobial activity. *Journal of Photochemistry and Photobiology B: Biology* **2016**, *163*, 77–86.